



WALKER DEPARTMENT OF MECHANICAL ENGINEERING
Nuclear Engineering Teaching Laboratory

Pickle Research Campus R-9000 • Austin, Texas 78758 • 512-232-5380 • FAX 512-471-4589
nuclear.engr.utexas.edu • wcharlton@austin.utexas.edu

February 9, 2023

ATTN: Document Control Desk
U. S. Nuclear Regulatory Commission
11555 Rockville Pike
Rockville, Maryland, 20852

Geoffrey Wertz, P.E.
Non-Power Production and Utilization Facility Licensing Branch (UNPL)
Division of Advanced Reactors and Non-Power Production and Utilization Facilities (DANU)
Office of Nuclear Reactor Regulation

SUBJECT: Docket No. 50-602, Facility Operating License R-129 - Submission of Neutronics Report and Thermal Hydraulic Analysis of the University of Texas (UT) TRIGA Reactor

REFERENCE: July 23, 2020 letter: University- of Texas at Austin – Regulatory Audit re: Renewal of Facility Operating License No. -129 (EPID No. L-2017-RNM-0032), (Agencywide Documents Access and Management System (ADAMS) Accession No. ML20203M166),

Sir:

We respectfully submit the *Analysis of the Neutronic Behavior of the Nuclear Engineering Teaching Laboratory Reactor at the University of Texas* and the *Thermal Hydraulic Analysis of the University of Texas (UT) TRIGA Reactor* in support of license renewal for the University of Texas at Austin as attached. If you have any questions, please contact me at 512-232-5373 or whaley@mail.utexas.edu.

P. M. Whaley

I declare under penalty of perjury that the foregoing is true and correct.

W. S. Charlton

ATT:

- (1) Analysis of the Neutronic Behavior of the Nuclear Engineering Teaching Laboratory at the University of Texas
- (2) Thermal Hydraulic Analysis of the University of Texas (UT) TRIGA Reactor

**ANALYSIS OF THE NEUTRONIC BEHAVIOR
OF THE
NUCLEAR ENGINEERING TEACHING LABORATORY REACTOR
AT
THE UNIVERSITY OF TEXAS**

Submitted By:

Radiation Center
Oregon State University
Corvallis, Oregon

February 2023

Table of Contents

1.	Introduction.....	4
2.	Summary and Conclusions of Principal Safety Considerations	4
3.	Reactor Fuel	4
4.	Reactor Core	6
5.	Model Bias	7
6.	Burnup Calculations.....	11
7.	Current Core Configuration	13
8.	Limiting Core Configuration	19
9.	Summary	24

List of Figures

Figure 1 – TRIGA® Stainless Steel Clad Fuel Element Design used in the NETL Core	5
Figure 2 – Schematic Illustration of the NETL Showing the Current Core Configuration	6
Figure 3 – Horizontal and Vertical Cross-sections of the NETL MCNP Model at BOL	7
Figure 4 – Reactivity (including bias) of 80 Different BOL Critical Core Configurations.....	8
Figure 5 – Reactivity (including bias) of 36 Different BOL Critical Core Configurations.....	9
Figure 6 – Vertical Cross-section of Current Core Configuration MCNP Model	13
Figure 7 – Current Core Power-Per-Element (in kW) Distribution at 1.1 MW	13
Figure 8 – Current Core Configuration Prompt Temperature Coefficient, α_F , as a Function of Temperature	16
Figure 9 – Current Core Configuration Moderator Void Coefficient.....	17
Figure 10 – Current Core Configuration Moderator Temperature Coefficient	17
Figure 11 – Vertical Cross-section of Limiting Core Configuration MCNP Model	19
Figure 12 – Limiting Core Configuration Power-Per-Element Distribution at 1.1 MW	20
Figure 13 – Limiting Core Configuration Prompt Temperature Coefficient, α_F , as a Function of Temperature	22
Figure 14 – Limiting Core Configuration Moderator Void Coefficient	22
Figure 15 – Limiting Core Configuration Moderator Temperature Coefficient.....	23

List of Tables

Table 1 – Characteristics of Stainless Steel Clad Fuel Elements.....	5
Table 2 – BOL Rod Worth Calculations.....	10
Table 3 – Summary of Burnup Steps.....	12
Table 4 – β_{eff} and Prompt Neutron Lifetimes for Current Core Configuration	14
Table 5 – Current Core Rod Worth Calculations.....	15
Table 6 – Current Core Configuration Prompt Temperature Coefficient.....	16
Table 7 – K-Effective Calculations Used to Determine Current Core Power Defect	18
Table 8 – β_{eff} and Prompt Neutron Lifetimes for Limiting Core Configuration.....	20
Table 9 – Limiting Core Configuration Rod Worth Calculations	21
Table 10 – Limiting Core Configuration Prompt Temperature Coefficient	22
Table 11 – K-Effective Calculations Used to Determine Limiting Core Power Defect.....	23
Table 12 – Limiting Core Hot Channel Power Summary.....	24

1. Introduction

This report contains the results of investigation into the neutronic behavior of the Nuclear Engineering Teaching Laboratory reactor (NETL) at the University of Texas Austin. The objectives of this study were to: 1) create a model of the NETL to study the neutronic characteristics, and 2) demonstrate acceptable reactor performance and safety margins for the NETL core under normal conditions.

2. Summary and Conclusions of Principal Safety Considerations

The conclusion of this investigation is that the MCNP model does an acceptable job of predicting behavior of the NETL core. As such, the results suggest that the current NETL core can be safely operated within the parameters set forth in the technical specifications. Discussion and specifics of the analysis are located in the following sections. The final sections of this analysis provide suggestions for a limiting core configuration.

3. Reactor Fuel

The fuel utilized in the NETL is standard TRIGA[®] fuel manufactured by General Atomics. The use of low-enriched uranium/zirconium hydride fuels in TRIGA[®] reactors has been previously addressed in NUREG-1282 [1]. This document reviews the characteristics such as size, shape, material composition, dissociation pressure, hydrogen migration, hydrogen retention, density, thermal conductivity, volumetric specific heat, chemical reactivity, irradiation effects, prompt-temperature coefficient of reactivity and fission product retention. The conclusion of NUREG-1282 is that TRIGA[®] fuel, including the fuel utilized in the NETL, is acceptable for use in reactors designed for such fuel.

The design of standard stainless steel clad fuel utilized in the NETL is shown in Figure 1. Stainless steel clad elements used at NETL all have fuel alloy length of 38.1 cm. The characteristics of standard fuel elements are shown in Table 1.

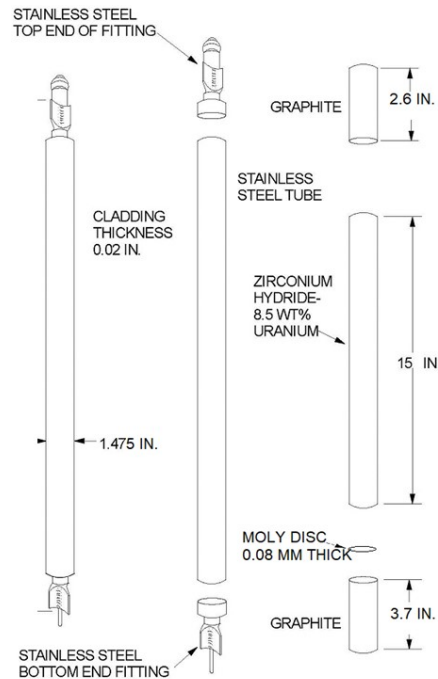


Figure 1 – TRIGA® Stainless Steel Clad Fuel Element Design used in the NETL Core

Table 1 – Characteristics of Stainless Steel Clad Fuel Elements

Uranium content [mass %]	8.5
BOL ²³⁵ U enrichment [mass % U]	19.75
Original uranium mass [gm]	37
Zirconium rod diameter [in]	0.25
Fuel meat outer diameter [in]	1.435
Cladding outer diameter [in]	1.475
Cladding material	Type 304 SS
Cladding thickness [in]	0.020
Fuel meat length [in]	15
Graphite slug outer diameter [in]	1.43
Upper graphite slug length [in]	2.6
Lower graphite slug length [in]	3.7
Molybdenum disc thickness [mm]	0.8

The NETL reactor initially achieved criticality in March of 1992, however all fuel (except for the fresh FFCRs) was previously used at other facilities. Most of it came from a previous reactor on campus at Taylor Hall, but there were other sources as well. This made the beginning-of-life (BOL) fuel isotopic determination difficult. UT Austin performed a SCALE analysis to burn the fuel in conjunction with the given burnup records. The SCALE outputs were used to create BOL fuel isotopics for the MCNP runs. However, the burnup records did not specify core location during previous irradiation, so these SCALE isotopics are a “best guess” given the previous information.

rods were based upon the manufacturing drawings. Representative cross-sectional views of the MCNP model (of the initial core loading) are shown in Figure 3.

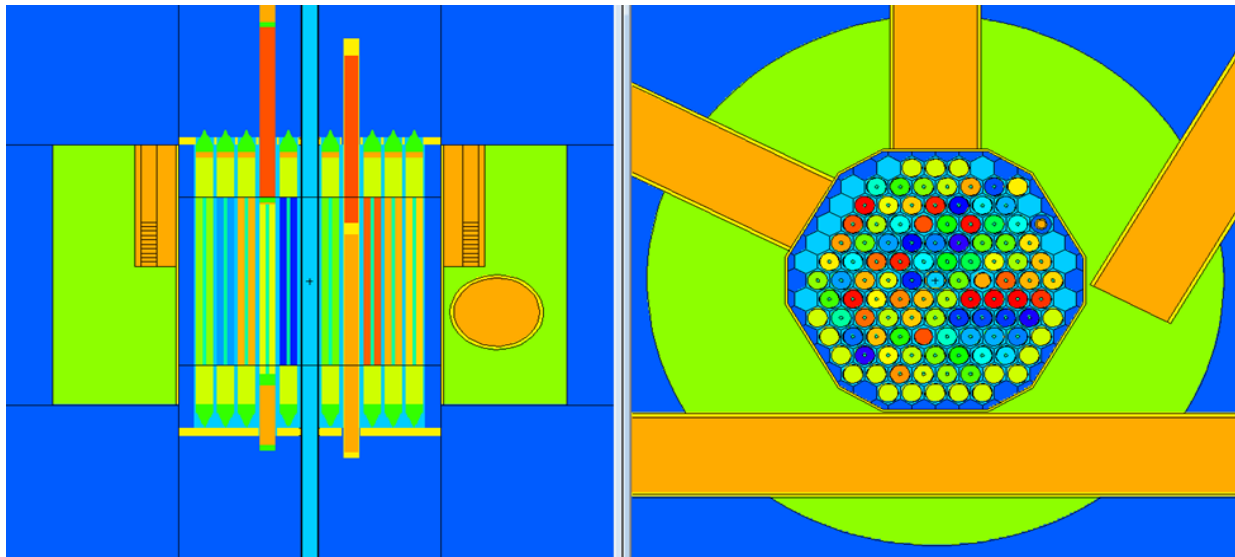


Figure 3 – Horizontal and Vertical Cross-sections of the NETL MCNP Model at BOL

5. Model Bias

Beginning-of-life Criticality Bias

Using critical rod height data from the first few months of NETL operation, a series of MCNP analyses based upon various critical rod heights were performed to determine the criticality bias of the model. This bias represents such things as differences in material properties that are difficult to determine or unknown (i.e., exact composition of individual fuel meats and trace elements contained therein) or applicability of cross section data sets used to model the reactor (i.e., interpolation between temperatures). As a result, the validation of the model was based upon the ability of the code to accurately predict criticality as compared with measurements made on the reactor in early 1992.

A criticality calculation was performed using cold clean critical core configuration information from 3/23/1992, which was the first time the NETL was taken to criticality. The k-effective of this configuration was 0.99393 ± 0.00013 , or $-\$0.87 \pm \0.04 . Eighty different critical core configurations were then analyzed to determine how they bounded around the bias of this initial critical configuration. Figure 4 shows these 80 configurations with respect to the bias run. All of these kcode calculations utilized 500,000 neutrons per cycle for 200 total cycles (175 active cycles).

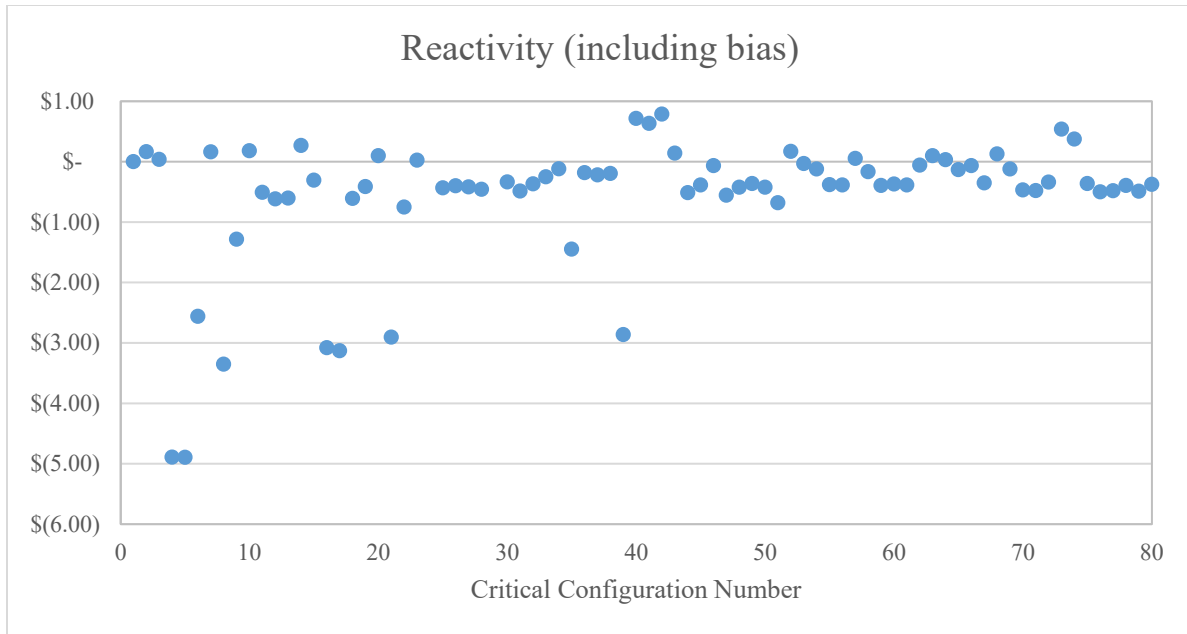


Figure 4 – Reactivity (including bias) of 80 Different BOL Critical Core Configurations

There appears to be significant deviation in the first 40 configurations. Note that most of these configurations are at low power (less than 100 W) but some are at high power (greater than 200 kW and the point of adding heat). Note that “low power” with respect to modeling means that the MCNP decks utilized cross section data files at ambient room temperature, and “high power” means that the decks utilized cross section data files at 600K (327 °C). Most of the configurations with significant deviation are the high power runs, which would indicate that either the model is inaccurate or there is evidence of another problem. One clue that there is a problem with the high power runs is the fuel temperature and critical rod heights. Some runs (like those on 3/23/92) listed reactor power around 400 kW, but fuel temperature only reads 20 degrees above ambient. There are also some criticality runs on 4/30/92 that produced an MCNP k-effective of approximately \$1.75, which may be indicative of a core that was not truly critical. For example, looking at the criticality state at 0944 on 4/30/92, the rods are at 0, 950, 481, and 488. At 1020, they are at 492, 950, 464, and 504. This does not make sense as the latter configuration has a rod that is 492 units removed while the other three rods are at essentially the same positions. The same occurrence can be seen at the timestamps at 1403 and 1407, where three rods are at the same heights but the transient rod is first at 396 units, then it is at 950 units.

If the first 44 runs are ignored (if runs after 5/1/92 are observed), the data looks more accurate (see Figure 5), with an average of $-\$0.23$. The decision to ignore the first 44 runs was not arbitrary; the reactor was not run above 1 kW from 5/1/92 until 7/1/92. Thus, the runs between these dates were a “cold clean core” and it would also appear that something happened between those dates to make the MCNP model more accurate, likely an improvement in reactor power measurement, which would improve the accuracy of the critical rod heights.

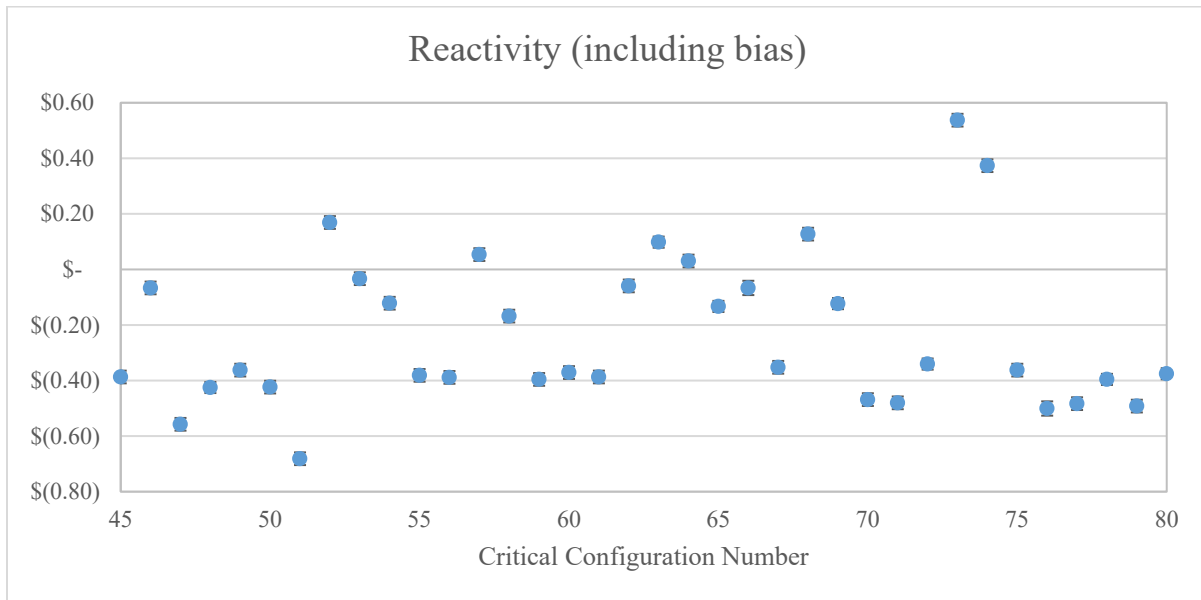


Figure 5 – Reactivity (including bias) of 36 Different BOL Critical Core Configurations

Note that these latter 36 configurations include some full power operations (cases #70-72, 76, 78 and 80). There is only one outlier over $\pm\$0.60$ (case #51), which would indicate that there were inconsistencies between high power operations during the first few months of operation. Other evidence, such as lower-than-expected fuel temperatures at these supposed high-power levels, would also indicate that something was inconsistent during the first few months of operation.

It is also important to note that some of these statistical outliers (e.g. cases #73 and #74) have unusual critical rod heights (0, 950, 950, 34 and 0, 855, 0, 950, respectively). It is possible that these having some control rods fully-withdrawn with others fully-inserted could be causing rod shadowing effects that are unable to be accurately simulated in MCNP.

Thus there are two aspects of the BOL criticality bias: the $-\$0.87$ initial criticality bias which is likely due to inaccurate BOL fuel isotopics, and a $-\$0.23$ bias that is mainly due to geometric

differences in the critical rod height configurations. As stated earlier, the bias represents such things as differences in material properties that are difficult to determine or unknown (i.e., lack of manufacturer mass spectroscopy data on the exact composition of individual fuel meats and trace elements contained therein) or applicability of cross section data sets used to model the reactor (i.e., interpolation between temperatures). A large source of error is the uncertainty of the contents of the BOL fuel meats, as all of the fuel (except for the FFCRs) was previously irradiated. Without knowing the exact burnup and previous grid location of these elements, it is nearly impossible to accurately determine their fuel compositions.

Beginning-of-Life Rod Worth Bias

NETL initially calibrated their control rods on 7/23/92. The control rod calibration procedure is listed in Appendix A. To simulate control rod calibrations in MCNP, two separate calculations were performed for each control rod. First, there are initial iterative attempts to achieve criticality by fully inserting the rod-to-be-calibrated and banking the other three rods at the same height until MCNP produces a k-effective near 1.0000. This simulates the initial state of the control rod calibration. Once this critical state is achieved, a second MCNP calculation is performed with the tested control rod fully withdrawn and all other parameters remaining the same. The difference between these two values is then simply the control rod worth. Table 2 shows a compilation of the MCNP-calculated rod worths compared to the NETL-measured control rod worths.

Table 2 – BOL Rod Worth Calculations

Control Rod	Full In	Full Out	MCNP Rod Worth	Experimental Worth	Difference
Transient	1.00047	1.02407	\$3.29	\$3.26	\$0.03
Regulating	1.00011	1.03067	\$4.24	\$4.08	\$0.16
Shim 1	0.99992	1.0238	\$3.33	\$3.04	\$0.29
Shim 2	1.00012	1.02419	\$3.36	\$3.17	\$0.19
All Rods Out (Core Excess)	N/A	1.04248	\$5.82	\$6.38	-\$0.56

MCNP appears to produce relatively reliable control rod worths. The control rod worth calculations are relatively close to the measured rod worths, especially the Transient and

Regulating rods, with the model correctly predicting that the Regulating rod would have the most worth. These two rods are in the C-ring, thus closer to the center of the core. It would make sense that their predictions are more accurate as there is generally more error as one goes further from the center of the core due to the diffusive nature of neutronics, which is typically less accurate the closer you get to a boundary, as well as albedo effects near the reflector at the edge of the reactor core. It is important to note that these reactivity values do not utilize the criticality bias numbers from the previous section, as that bias would be moot, since these k-effective values are relative to one another.

MCNP under-predicts the core excess reactivity by \$0.56, which coincides with the -\$0.87 reactivity bias. It would appear that the BOL fuel isotopics may have been “over-burned” by the SCALE calculations, but as stated earlier, it is nearly impossible to determine the accuracy of the BOL fuel isotopics without knowing the fuel’s previous geometry during burnup.

Bias Conclusion

The criticality bias and the rod worth bias calculations would appear to demonstrate that the MCNP model is relatively accurate with respect to geometry but is hampered by the inaccurate BOL fuel isotopics. The 44 critical core configuration bias calculations average of -\$0.23 is relatively accurate considering that unknown fuel isotopics and rod shadowing effects could be causing general inaccuracies. The rod worth calculations predicted the most valuable control rod, reliably predicted the Transient Rod worth, and was still relatively accurate with regards to the Shim 1 and Shim 2 rod worths.

6. Burnup Calculations

MCNP has a “BURN” option, which causes MCNP to invoke the CINDER90 code for depletion simulations. CINDER90 has an inventory of over 3400 nuclides and is compatible with MCNP. This option requires the user to specify a time step (in days), a power fraction (typically 100% or 1.0), power level (in MW), and the materials that are to be depleted.

After performing the initial model bias calculations, a series of MCNP BURN calculations were performed to burn the NETL fuel to its current core configuration which was established in February 2018. This was a very detailed process as NETL is a very active facility and experienced

many different core configurations. Using the fuel move logs, it was determined that there were 18 significant different core configurations that needed to be modeled (see Table 3).

Each burnup step involved performing the fuel burnup for the specified amount of MW-days, which is a computationally expensive task, often requiring 24 hours to perform each step depending on cluster node usage. After the burnup calculation is completed, the output fuel isotopics were parsed, then the core model was reconfigured and the relevant fuel isotopics were pasted into the model and the next burnup step was performed.

Table 3 – Summary of Burnup Steps

Burnup Step	From	To	MW-days	Total MW-days	FEs	Note
1	3/19/1992	10/12/1995	9.201	9.201	87	Initial Fuel Load
2	10/12/1995	1/20/1998	5.276	14.477	87	New IFE
3	1/20/1998	6/19/1998	2.789	17.266	87	Fuel Swapped Out/Add Rabbit
4	6/19/1998	3/4/1999	6.376	23.642	87	New IFE
5	3/4/1999	11/12/1999	7.671	31.313	90	Add 3 Fuel Elements
6	4/6/2000	6/29/2000	3.444	34.757	89	Core Reload
7	6/29/2000	1/29/2001	1.919	36.676	92	3L Experiment
8	1/29/2001	7/30/2001	9.138	45.814	92	3L Experiment with New IFE
9	7/30/2001	7/22/2002	21.508	67.322	95	Add 3 Fuel Elements
10	7/22/2002	11/13/2002	13.966	81.288	95	Fuel Shuffle
11	11/13/2002	4/1/2004	24.933	106.221	103	Add 8 New Fuel Elements
12	7/26/2004	7/13/2005	15.71	121.931	102	3L Experiment Core Reload
13	7/13/2005	7/11/2006	22.983	144.914	104	Add 2 Fuel Elements
14	7/11/2006	7/24/2007	41.732	186.646	104	Fuel Shuffle
15	7/24/2007	6/12/2008	18.347	204.993	108	Add 4 Fuel Elements
16	6/12/2008	6/24/2010	21.288	226.281	110	7L Experiment
17	6/24/2010	1/15/2016	73.587	299.868	114	Remove 7L Experiment
18	1/15/2016	2/22/2018	38.026	337.894	114	New IFE

The red highlighting indicates the hottest fuel element locations, which are in B-1 and B-2, with a maximum power of 15.93 kW (at a total maximum core power of 1.1 MW). B-2 is actually slightly higher than B-1 (15.931 kW vs. 15.929 kW) but both are within the 2-sigma error of 0.04 kW.

Effective Delayed Neutron Fraction and Prompt Neutron Generation Time

MCNP outputs effective delayed neutron fraction (β_{eff}) and prompt neutron lifetime when using the KOPTS card. Nine different MCNP calculations (the same calculations used in the following Core Excess section) were used to determine β_{eff} and prompt neutron lifetime (see Table 4).

Table 4 – β_{eff} and Prompt Neutron Lifetimes for Current Core Configuration

Case	Prompt Neutron Generation Time (s)	Error (s)	β_{eff}
Trans fully in	47.62	7.543	0.00705
Trans fully out	46.868	7.111	0.00716
Reg fully in	48.08	7.824	0.00707
Reg fully out	46.718	6.961	0.00707
Shim I fully in	48.023	7.748	0.00702
Shim I fully out	46.777	6.974	0.00705
Shim II fully in	48.104	7.684	0.00717
Shim II fully out	46.708	7.086	0.00713
All Rods Out	45.824	6.626	0.00720
Average	47.191	7.284	0.00710

The average effective delayed neutron fraction β_{eff} was calculated to be 0.00710 ± 0.00007 . This is in reasonable agreement with values predicted in other LEU TRIGA[®] cores (i.e., Oregon State University $\beta_{\text{eff}} = 0.0076$ [3], University of Maryland $\beta_{\text{eff}} = 0.007$ [4]) and also the value historically used for the NETL of $\beta_{\text{eff}} = 0.007$. The value $\beta_{\text{eff}} = 0.007$ will be used to express all dollar values of reactivities in this report.

The average prompt neutron generation time is 47.191 ± 7.284 seconds.

Core Excess, Control Rod Worth and Shutdown Margin

Nine different MCNP calculations were performed to determine core excess, control rod worth, and shutdown margin. Core excess is calculated as the reactivity of all rods withdrawn from the core. Control rod worths and shutdown margin were calculated by determining a critical state of the reactor with one rod full inserted and the other three rods banked at the same height, then fully withdrawing the previously-inserted rod. The resulting values (with comparison to values measured at NETL) are shown in Table 3.

Table 5 – Current Core Rod Worth Calculations

Case	MCNP k-effective Rod Full-In	MCNP k-effective Rod Full-Out	MCNP Rod Worth	Experimental Reactivity	Difference
Transient	1.00035	1.02354	\$3.24	\$3.44	-\$0.20
Regulating	0.99978	1.02214	\$3.13	\$3.18	-\$0.05
Shim 1	1.00078	1.02248	\$3.03	\$3.09	-\$0.06
Shim 2	1.00014	1.0211	\$2.93	\$2.94	-\$0.01
All Rods Out (Core Excess)	-	1.04118	\$6.75	\$6.06	\$0.69

MCNP appears to accurately calculate the individual rod worths. The Regulating, Shim 1 and Shim 2 rods are all within the margin of error (which is approximately $\pm\$0.06$ for each case).

These calculations show a core excess of $\$6.75 \pm \0.03 . This is below the technical specification limit of $\$7.00$. The core excess was measured by NETL to be $\$6.06$ on 3/6/18. MCNP appears to have over-estimated core excess by approximately $\$0.70$. This could be due to a variety of reasons, such as only modeling the fuel elements as one single material per element, thus some burnup resolution is lost as the fuel does not burn uniformly throughout.

The technical specification definition of shutdown margin is “the minimum reactivity necessary to provide confidence that the reactor can be made subcritical by means of the control and safety systems starting from any permissible operating condition (the highest worth MOVEABLE EXPERIMENT in its most positive reactive state, each SECURED EXPERIMENT in its most reactive state), with the most reactive rod in its most reactive position, and that the reactor will remain subcritical without further operator action.” The most reactive rod is the Transient rod.

Total rod worth minus the Transient rod is $\$9.09 \pm \0.06 . NRC shutdown margin is this value minus the core excess, which would be $\$2.34 \pm \0.06 , which is far above the technical specification limit of $\$0.29$.

Prompt Fuel Temperature Coefficient

The prompt-temperature coefficient associated with the NETL fuel, α_F , was calculated by varying the fuel meat temperature while leaving other core parameters fixed. The MCNP model was used to simulate the reactor with all rods out at 293, 600, 900, 1200 and 2500 K. The prompt-temperature coefficient for the fuel was calculated at the mid-point of the four temperature intervals. The results are shown in Figure 8 and tabulated in Table 5. Results from GA were added to show similarity [5]. The prompt-temperature coefficient is observed to be negative for all evaluated temperature ranges with decreasing magnitude as temperature increases. The coefficient has a value of $-1.3\text{¢}/^\circ\text{C}$ at 446.8 K, which is similar to the value of $-\$0.01/^\circ\text{C}$ stated in the original SAR [6].

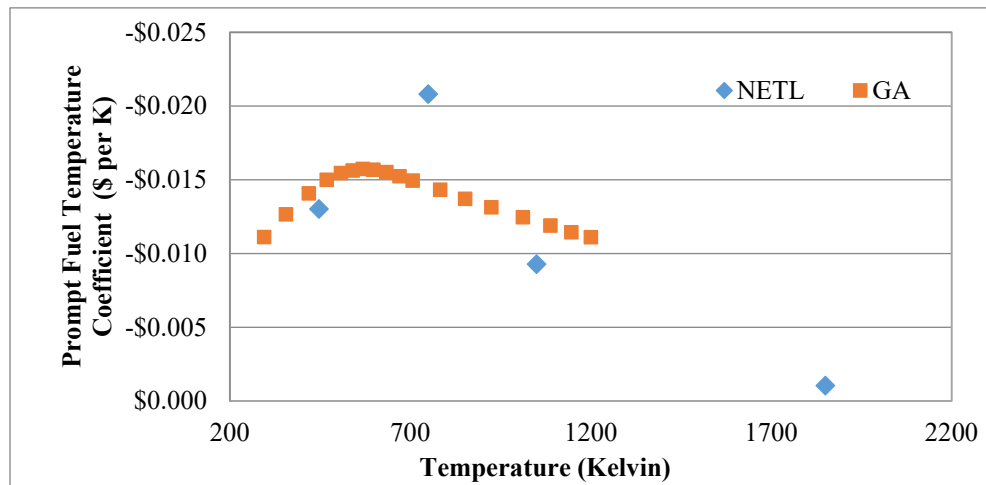


Figure 8 – Current Core Configuration Prompt Temperature Coefficient, α_F , as a Function of Temperature

Table 6 – Current Core Configuration Prompt Temperature Coefficient

Fuel Temperature [K]	Prompt Temperature Coefficient [$\$/^\circ\text{C}$]
446.8	-\$0.0130
750	-\$0.0208
1050	-\$0.0092
1850	-\$0.0010

Moderator Void Coefficient

The moderator void coefficient of reactivity was also determined using the MCNP model. The voiding of the core was introduced by uniformly reducing the density of the liquid moderator in the entire core. The calculation was performed from 0% to 100% voiding at 10% intervals. The void coefficient was negative for every interval and steadily decreased, as can be seen in Figure 9.

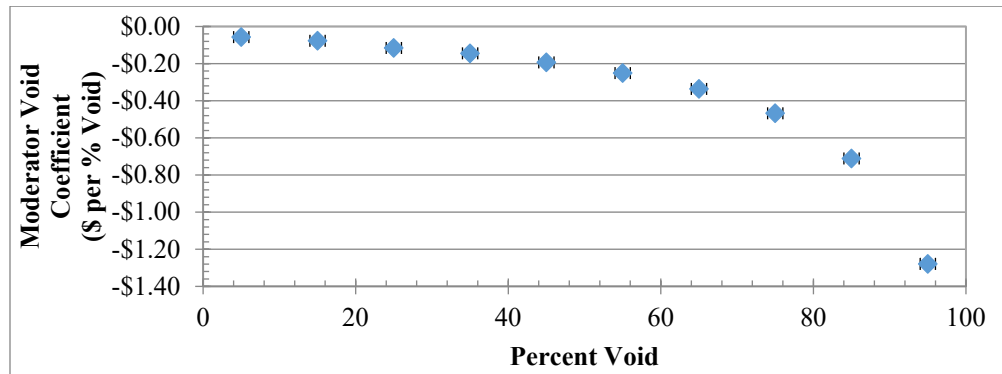


Figure 9 – Current Core Configuration Moderator Void Coefficient

Moderator Temperature Coefficient

The moderator temperature coefficient of reactivity, α_M , was determined by varying the moderator density with respect to temperature within the MCNP model from the expected operating temperature range of 20°C to 50°C (using Engineering Toolbox [7] to determine water density). The results are shown in Figure 10. The moderator temperature coefficient is calculated to be slightly positive from 25°C to 30 °C and from 45 °C to 50 °C, but these changes are less than \$0.01/°C and both points (with 2-sigma error) are bounded around zero. The moderator temperature coefficient appears to be negligible.

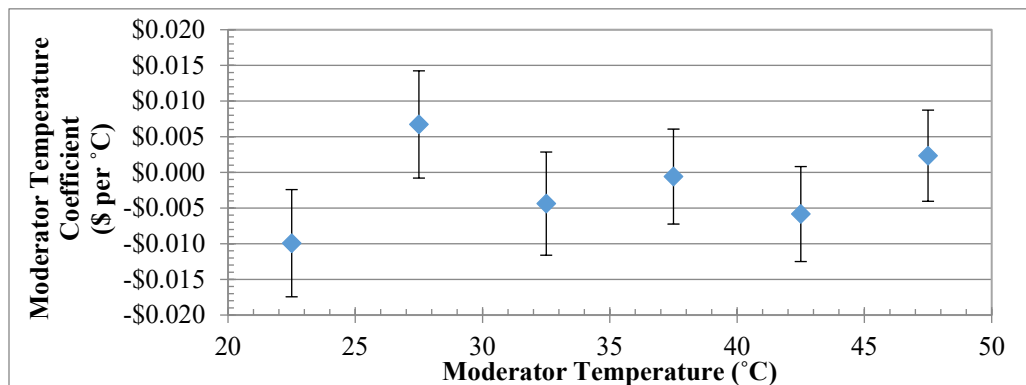


Figure 10 – Current Core Configuration Moderator Temperature Coefficient

Power Coefficient of Reactivity

The power coefficient of reactivity, otherwise known as power defect, is the amount of reactivity required to overcome the temperature feedback during the rise to power. This is modeled by analyzing two MCNP decks that are similar except for the neutron cross-sections used. Two k-effective calculations were performed with all rods out, one using cross sections at 293K (low power) and one using cross sections at 600K (full power). The results are seen in Table 6.

Table 7 – K-Effective Calculations Used to Determine Current Core Power Defect

Case	MCNP k-effective	Standard Deviation	Reactivity	Error (2-sigma)
Low Power	1.04118	0.00012	\$6.75	\$0.03
Full Power	1.01327	0.00010	\$2.94	\$0.03

Power defect is simply the difference in reactivity between these two cases; thus the power defect is $\$3.81 \pm \0.05 .

8. Limiting Core Configuration

This section will suggest a limiting core configuration that utilizes fresh fuel to improve reactor efficiency while maintaining proper safety margins. The NETL limiting core configuration is a core that completely consists of fresh fuel.

Figure 11 shows the suggested limiting core configuration. For this analysis, it is suggested that the core is loaded with 84 fresh fuel elements (including FFCRs), which will provide just under the license limit of \$7.00 core excess ($\$6.93 \pm \0.07). This is comparable to the original 1992 BOL core configuration, which was measured to have a \$6.38 core excess on a core of 87 lightly-irradiated fuel elements. This configuration will provide maximum flux to the beam port facilities while maintaining safety margins.

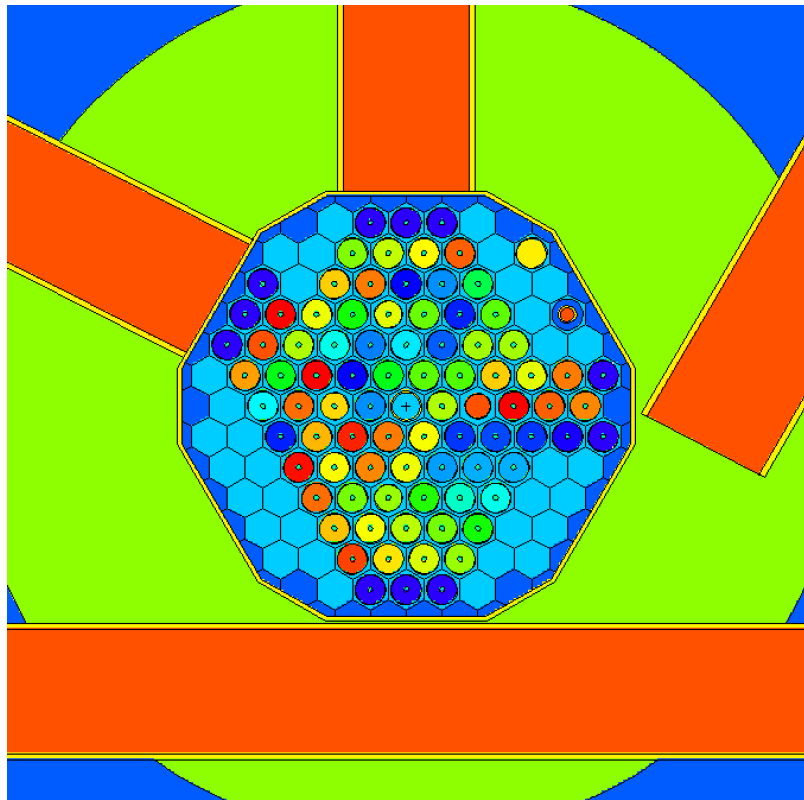


Figure 11 – Vertical Cross-section of Limiting Core Configuration MCNP Model

The average β_{eff} was calculated to be 0.00735 ± 0.00007 . There is a slight increase in β_{eff} compared to the current core configuration, but for consistency, 0.007 will continue to be used to express all dollar values of reactivities in this report.

The average prompt neutron generation time is 42.791 ± 5.265 seconds.

Core Excess, Control Rod Worth, and Shutdown Margin

The same nine MCNP rod worth calculations were performed again for the limiting core configuration: Core excess, shutdown margin, and individual rod worths were calculated from these outputs and the reactivity values (with the bias taken into account) of each of these calculations are shown in Table 7.

Table 9 – Limiting Core Configuration Rod Worth Calculations

Case	MCNP k-effective Rod Full-In	MCNP k-effective Rod Full-Out	MCNP Rod Worth
Transient	0.99886	1.02191	\$3.22
Regulating	1.00024	1.03222	\$4.43
Shim 1	1.00003	1.02431	\$3.39
Shim 2	1.0003	1.02857	\$3.93
All Rods Out (Core Excess)	-	1.04257	\$6.93

These calculations show a core excess of $\$6.93 \pm \0.07 . This is below the technical specification limit of \$7.00.

Now the most reactive rod is the Regulating, due to having more fuel near its vicinity and the power shifted to the northwest side of the core. Total rod worth minus the Regulating Rod is $\$10.53 \pm \0.16 . NRC shutdown margin is this value minus the core excess, which would be $\$3.60 \pm \0.16 , which is still far above the technical specification limit of \$0.29.

Prompt Fuel Temperature Coefficient

The results of the limiting core configuration prompt fuel temperature coefficient calculations are shown in Figure 13 and tabulated in Table 9.

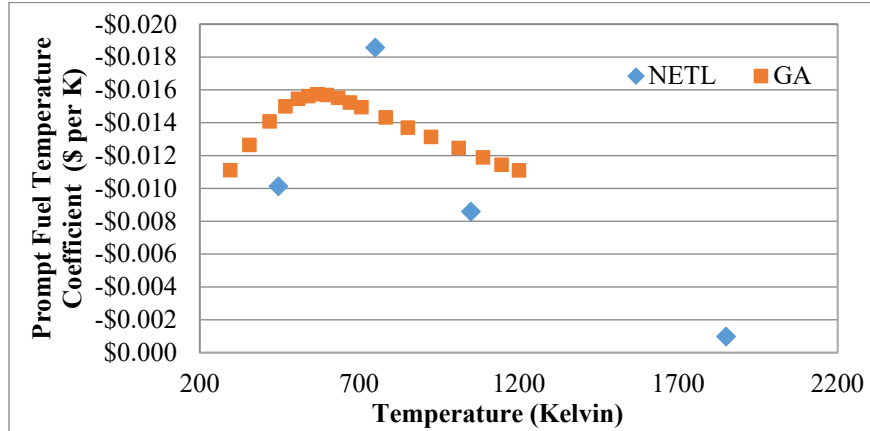


Figure 13 – Limiting Core Configuration Prompt Temperature Coefficient, α_F , as a Function of Temperature

Table 10 – Limiting Core Configuration Prompt Temperature Coefficient

Fuel Temperature [K]	Prompt Temperature Coefficient [\$/°C]
446.8	-\$0.01014
750	-\$0.01858
1050	-\$0.00860
1850	-\$0.000989

These values are slightly higher than the original BOL coefficients, likely due to the fresh fuel.

Moderator Void Coefficient

Figure 14 shows the moderator void coefficient in the suggested limiting core configuration.

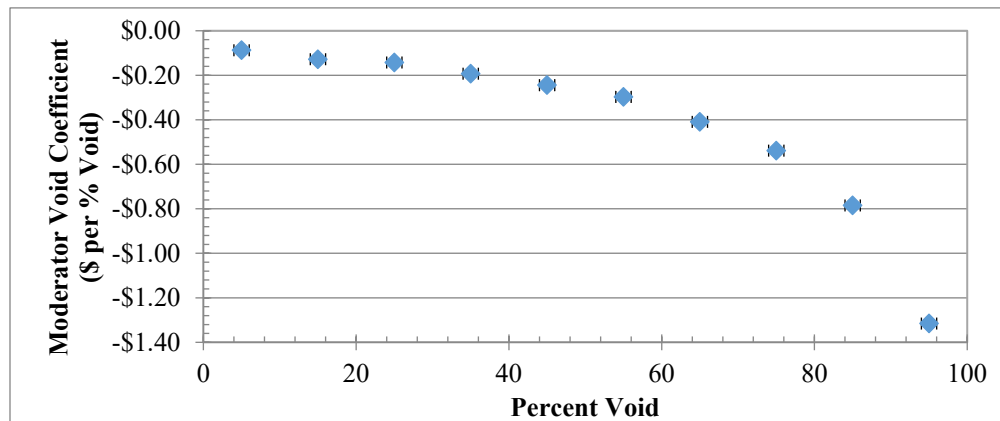


Figure 14 – Limiting Core Configuration Moderator Void Coefficient

The void coefficient was negative for every interval and steadily decreased, similar to the current core configuration. The void coefficient is slightly more negative in the limiting core configuration, likely due to having more moderator in the core configuration.

Moderator Temperature Coefficient

Figure 15 shows the moderator temperature coefficient in the suggested limiting core configuration.

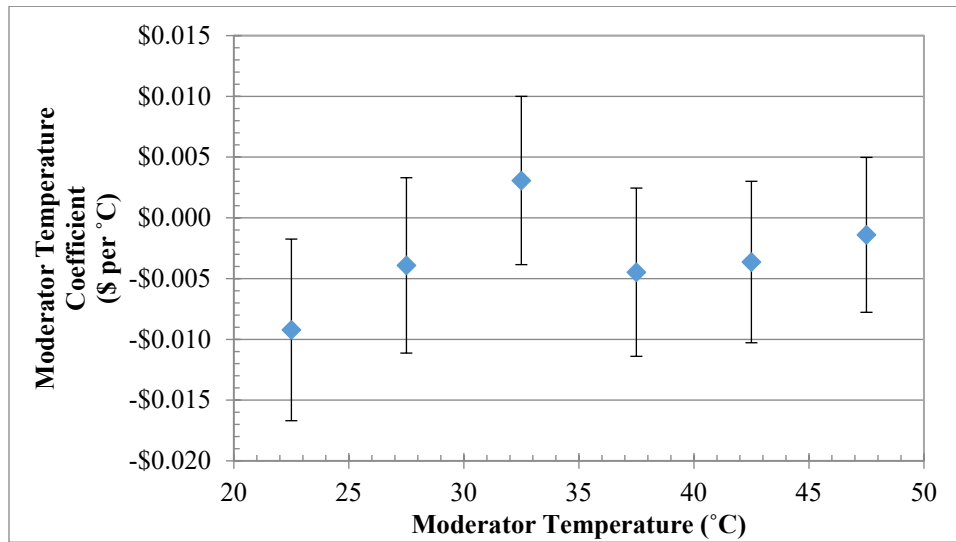


Figure 15 – Limiting Core Configuration Moderator Temperature Coefficient

Once again the moderator temperature coefficient appears to be negligible as it bounds around \$0.00 at nearly all observed temperature ranges.

Power Coefficient of Reactivity

The power coefficient of reactivity results are seen in Table 10.

Table 11 – K-Effective Calculations Used to Determine Limiting Core Power Defect

Case	MCNP k-effective	Standard Deviation	Reactivity	Error (2-sigma)
Low Power	1.04231	0.00015	\$6.90	\$0.04
Full Power	1.01921	0.00010	\$3.79	\$0.03

Thus the power defect is 3.11 ± 0.05 . This is lower than the current core configuration's power defect, likely due to less resistance at the point-of-adding-heat due to the lower amount of zirconium-hydride in the core.

Hot Channel Power Summary

The hot channel in the limiting core configuration was determined to be B-5. An fmesh calculation was performed to analyze a 20 by 20 mesh array to determine axial and radial power distributions. Table 11 summarizes the results of this calculation.

Table 12 – Limiting Core Hot Channel Power Summary

Core Configuration	Hot Rod Location	Hot Rod Thermal Power [kW]	Hot Rod Peak Factor [P_{max}/P_{avg}]	Hot Rod Axial Peak Factor [P_{max}/P_{avg}]	Hot Rod Radial Peak Factor [P_{max}/P_{avg}]	Effective Peak Factor
Limiting Core	B6	22.14	1.691	1.296	1.017	2.229

9. Summary

MCNP6.2 was used to calculate fundamental and operational parameters for the Nuclear Engineering Teaching Laboratory Reactor to demonstrate the reactor's adherence to safety margins in the technical specifications. Values of fundamental parameters agree well with theoretical values. Values of operational parameters agree well with measured values, giving confidence in the model's ability to predict the viability of future core configurations. The results of this study indicate that the NETL can be operated safely within the Technical Specification bounding envelope and that its MCNP model can be used to predict future core configuration changes.

REFERENCES

- [1] NUREG-1282, "Safety Evaluation Report on High-Uranium Content, Low-Enriched Uranium-Zirconium Hydride Fuels for TRIGA[®] Reactors,' USNRC, August 1987.
- [2] C.J. Werner, et al., "MCNP6.2 Release Notes", Los Alamos National Laboratory, report LA-UR-18-20808 (2018).
- [3] "Safety Analysis Report for the Conversion of the Oregon State University TRIGA[®] Reactor from HEU to LEU Fuel," Submitted by the Oregon State University TRIGA[®] Reactor (2007).
- [4] "Analysis of the Neutronic Behavior of the Maryland University Training Reactor," Submitted by the Oregon State University Radiation Center to the Department of Energy (July 2017).
- [5] GA-7882, Kinetic Behavior of TRIGA[®] Reactors, General Atomics (1967).
- [6] "Safety Analysis Report" Submitted by the University of Texas at Austin Nuclear Engineering Teaching Laboratory (January 2012).
- [7] Engineering Toolbox. Web. Accessed May 3rd, 2017.
Link: http://www.engineeringtoolbox.com/water-thermal-properties-d_162.html

APPENDIX A – NETL Control Rod Calibration Procedure

PROCEDURE

SURV-6

Control Rod Calibration

Version

1.00

Approvals:

Steve Buehler

Facility Director, NETL

3/2/09

Date

Richard M. [Signature]

Chairperson, Nuclear Reactor Committee

3/2/09

Date

Number of Pages: 8
Number of Words: 2396
Number of Characters: 11929

NUCLEAR ENGINEERING TEACHING LABORATORY
J. J. PICKLE RESEARCH CAMPUS
THE UNIVERSITY OF TEXAS AT AUSTIN

or drive maintenance, reactor core reconfiguration, or movement of fuel adjacent to the standard rod drives.

D. Contents

- A. Rod Drop Procedure page 4
- B. Positive Period Procedure page 5
- C. Control Rod Drop Time and Removal Rate Measurement page 7

E. Attachments

- 1. Reactivity vs. Power Ratio Plot 1 Page
- 2. Positive Period Data Sheet 1 Page
- 3. Stable Period Wait Time 1 Page
- 4. Inhour curve - Reactivity vs. Period Plot 1 Page
- 5. Rod Drop Time / Withdrawal Rate Data Sheet 1 Page

F. Equipment, Materials

TRIGA ICS System with control rod drives
 Data Analysis Software such as "MathCAD"
 Digital Stopwatch
 Digital Storage Oscilloscope

G. References, Other Procedures

MAIN-6, Rod & Drive Maintenance, Inspection
 Attachments 1 & 3 :
 A. Edward Profio, "Experimental Reactor Physics", John Wiley and Sons
 Inc., 1976, pp 712, 716
 Attachment 4 :
 General Atomics Data Sheet.

Date of Change: _____
 Change Approval: _____
 NETL Director

Stamp (Original-Red, Copy-Blue)

COPY

II. PROCEDURE

A. Control Rod Worth Estimate by Rod Drop Method:

Use to estimate initial control rod worth following new core start-up. May be useful following substantial core reconfigurations.

- 1. The reactor core condition should be cold and clean prior to measurement of rod worth. Perform ICS system pre-start checks. The reactor coolant system pumps should be off during control rod calibration.
2. Commence Startup of the reactor:
a. Position the control rod being evaluated at the desired position - full up if the entire rod worth is desired to be estimated in one step, or partially withdrawn at selected increasing withdrawn locations if several drops are to made.
b. Position the two rods closest to the rod being evaluated at a banked elevation, position the control rod farthest from the rod being calibrated at about 900 units to allow fine control of its reactivity for achieving criticality.
c. Adjust control rods for criticality at a low power level such as 50 to 500 watts. The power should not be so high as to see a fuel temperature increase above ambient i.e. less than 1 Kilowatt.
d. Remove the neutron source and readjust for criticality. The delayed neutrons should be allowed to come into equilibrium as evidenced by the indicated power remaining constant to within +/- 2% for a minimum of 3 to 5 minutes without further rod movement.
3. Setup data recording system to record reactor linear power as a function of time or use stopwatch and indication on linear power display to tabulate initial power and the indicated power after the control rod is dropped.
4. Drop control rod being evaluated by actuation of magnet button (standard rod drives) or air button (transient rod drive) and document the power vs. time data. Select times to record data based on time data plotted on the graph in Attachment 1 - Ratio of neutron density after a rod drop to the initial density (at critical), as a function of subcritical reactivity.

Date of Change:
Change Approval
NETL Director

Stamp (Original-Red, Copy-Blue)

COPY

- 5. Using the data in Attachment 1, determine the reactivity associated with the rod drop based on the measured neutron density ratio (power ratio) at the specified time after the rod drop.

B. Control Rod Worth Measurement by Positive Period Method:

Use for the annual rod worth calibration.
 Use as the primary rod calibration method.

- 1. The reactor core condition should be cold and clean prior to measurement of rod worth. Perform ICS system pre-start checks. The reactor coolant system pumps should be off during control rod calibration.
- 2. Commence Startup of the reactor:
 - a. Position the control rod being evaluated at the desired position – full down if the entire rod worth is to be evaluated, or at predetermined locations if the shape of the differential rod worth curve has already been established.
 - i. Initial control rod calibrations or calibrations after major core reconfigurations should evaluate the entire rod worth by stepwise pulling the rod in increments correlating to reactivity steps of 15 to 20 cents over its entire travel. This will require taking 10 to 20 measurements per control rod depending on its total worth.
 - ii. Once the initial control rod calibration curve shape has been established, subsequent routine control rod calibrations may be made by using only 5 or 6 appropriately selected insertions of the same reactivity magnitude as above. One or two points should be selected near the rod height correlating to the peak differential rod worth. Four additional points should be selected, two in the lower and two in the upper parts of the rod travel correlating to areas spaced roughly equally on the slope portions of the differential worth curve. The data from these measurements can then be curve fit to the shape of the differential control rod worth curve to determine the actual rod worth.
 - b. Position the two rods closest to the rod being evaluated at a banked elevation, position the control rod farthest from the rod being calibrated at about 900 units to allow fine control of its reactivity for achieving criticality.
 - c. Adjust control rods for criticality at a low power level of 1 to 3 Watts.

Date of Change: _____
 Change Approval _____
 NETL Director _____

Stamp (Original-Red, Copy-Blue)

COPY

3. Remove the neutron source and readjust for criticality. The delayed neutrons should be allowed to come into equilibrium as evidenced by the indicated power remaining constant to within +/- 4% for a minimum of 3.5 to 5 minutes without further rod movement. This constraint will limit measurement errors of criticality to +/- ~0.25¢ per measurement.
4. Record the Control rod positions on the Control Rod Calibration Data Sheet in Attachment 2.
5. Pull the control rod being calibrated in one smooth movement a distance correlating to an estimated reactivity worth of 15 to 20 cents which correlates to a stable period between 58 and 37 seconds. Record the rod position stop point on data sheet. (To minimize rod position hysteresis, if you inadvertently pull the rod too far, quickly move the rod back down slightly below the target point, then raise the rod to the target point.) Refer to previous calibration data to estimate the number of units to move the rod. Typical movements are 90 to 100 units for the initial and final pull at the full down or full up endpoints, decreasing rapidly to 20 to 40 units per pull in the mid range of rod travel. The reactivity per pull is limited to allow the reactor to attain a stable period prior to taking the power vs. time data thus reducing measurement errors. The time to reach a stable period is called the wait time. The wait times for 5% error are 20 to 35 seconds, for a 1% error they increase to 50 to 65 seconds respectively for 37 to 58 second stable periods. A table showing measurement errors as a function of the wait time required to attain a stable period is shown in Attachment 3.
6. Observe the power increase as indicated on the digital readout of the auto ranging linear power channel on the Animation Window. Use a stopwatch set to measure time intervals with respect to the start time. Start the primary stopwatch when the power passes the 60 watt point. Record the time when the power passes the 90 watt level, the 600 watt level, and the 900 watt level (time points should be marked at the first instant the power reaches the target value on the digital display). Time data at powers above the 1 Kilowatt level shall not be used as temperature feedback will create errors above this level.
7. Drive control rods other than the rod being calibrated down to decrease the reactor power. Leave the control rod being calibrated at the point to which it was withdrawn in step 5 if the entire rod is being stepwise calibrated. If the curve fit method is being used, reposition the rod being calibrated to its next starting point.
8. Repeat steps 2 through 7 until the remainder of the rod is completed or sufficient data points for curve fitting are obtained.

Notes: As long as the power level is not allowed to fall below the source interlock the source may be continuously left out of the core until all the data points desired are obtained.

Date of Change: _____
 Change Approval _____
 NETL Director _____

Stamp (Original-Red, Copy-Blue)

COPY

Each sequence through this process will take approximately 15 minutes if everything is done with attention to detail so plan accordingly.

9. Analyze data either manually or via software program. Using the time data recorded, calculate the stable period resulting from each rod pull. Then use the reactivity equation or inhour curve in Attachment 4 to determine the reactivity associated with each rod pull.
10. A senior operator should review and approve the rod calibration data. If significant changes in rod worth are indicated, a review of the implications on excess reactivity and shutdown margins should also be initiated.

C. Control Rod Withdrawal, insertion, and drop time measurements.

1. Perform ICS system pre-start checks if not already completed.
2. Setup drop time measurement system. The magnet power supply voltage level controlled by the console scram switch should be used to start the timing. A signal from the control rod down limit switch should be monitored to indicate when the rod has reached the full down position
 - a. Measurement equipment should be a storage oscilloscope or an electronic timer with signal start-stop features. Use of a stopwatch to measure rod drop time, manually started at the time the scram button is depressed and stopped at the time the rod visually hits bottom is also acceptable but not the preferred method of measurement.
 - b. Measurement resolution for oscilloscope sweep should be set to 100 ms/div, vertical gain should be set to 5 V/div. Vertical signal probe should be set to X 10 for the transient rod, and X 1 for all other rods. Scope should be set to Auto trigger mode while setting up, and changed to single trigger or normal mode when taking the data.
 - c. Connect start signal (scope trigger) to the Regulating rod positive magnet power (see table below for connection location). Set the scope trigger to DC coupling on a negative slope at a level of about 10 volts. The nominal magnet power high side is +13 volts and the low side is -6volts.
 - d. Connect the signal (Channel 1) to the rod drive down limit switch (see table below for connection location) of the drive being evaluated.

<i>Scope Input Channel</i>	<i>DAC Tie Bar</i>	<i>Description</i>
Trigger	TB 5-3	Reg Magnet Pwr (+13V)
CH 1	TB 8-8	TR rod down limit
CH 1	TB 8-16	Shim 1 rod down limit
CH 1	TB 8-24	Shim 2 rod down limit
CH 1	TB 9-32	Reg rod down limit

Date of Change: _____
 Change Approval _____
 NETL Director _____

Stamp (Original-Red, Copy-Blue)

1
2
3
4
5
6
7
8
9
10
11
12
13
14
15
16
17
18
19
20
21
22
23
24
25
26
27
28

- 3. Withdraw control rod being measured about 60 units and test drop the rod to verify the scope setup.
- 4. Fully withdraw the rod being evaluated, measuring the time it takes to move from full down to full up using a stopwatch. Record data on Attachment 5.
- 5. Drop the control rod to trigger and record a trace by initiation of the scram button. Drop time is measured from the time the scope triggered until the rod reaches full down, as evidenced by the transition of the signal on the rod down switch. Some rods may show a bounce after the initial bottom transition, typical drop time recorded is the time measured to when the rod remains full down as indicated on the trace. Record data on Attachment 5.
- 6. Repeat steps 2d through 5 for each remaining rod.
- 7. Calculate measured reactivity insertion rate and record data on Attachment 5:
 - a.. Obtain peak differential rod worth near rod midpoint for each rod from the control rod calibration data.
 - b. Calculate insertion rate (< 0.2 % Δk/k/sec) as follows:

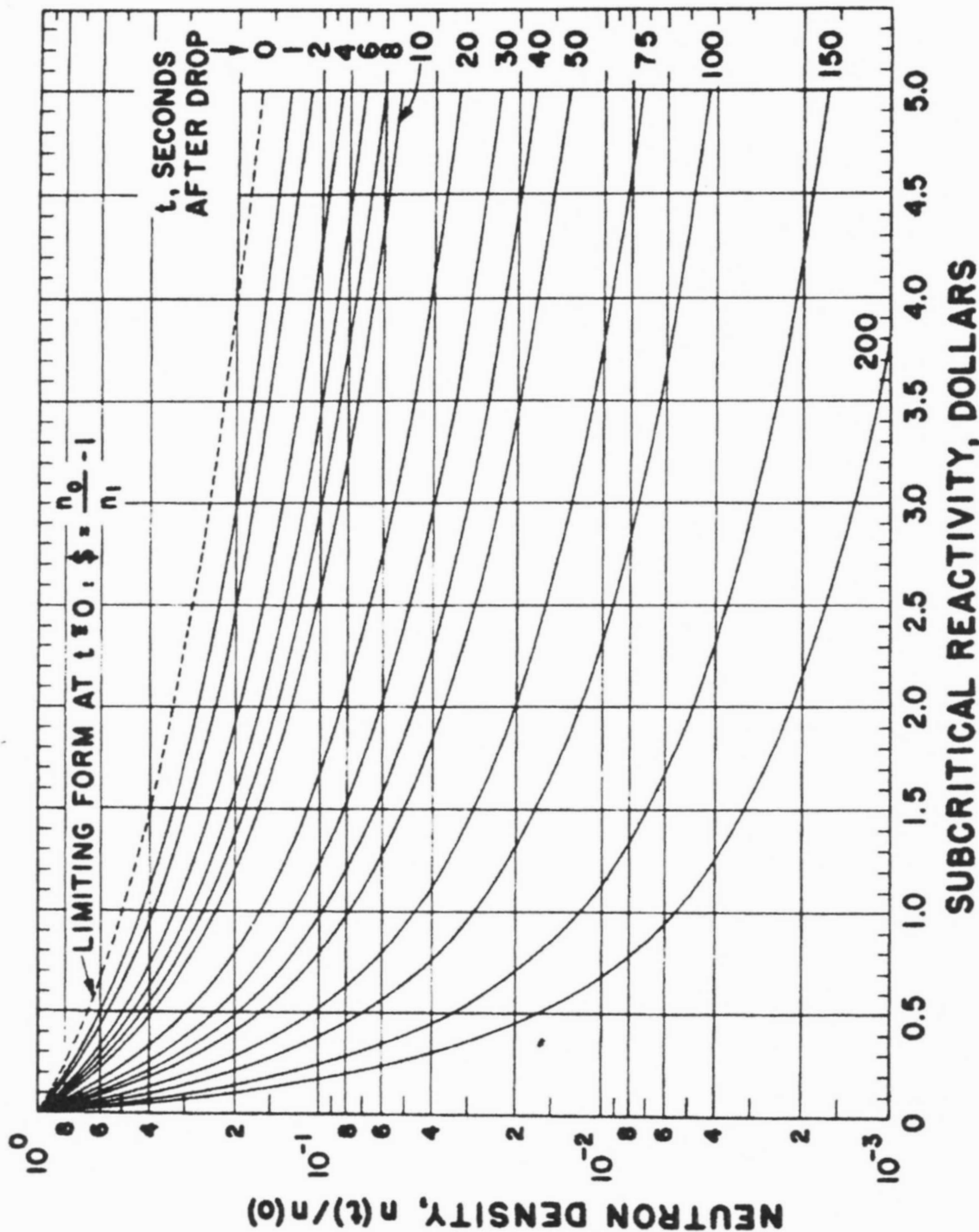
$$\text{rate (\% } \Delta k/k/\text{sec)} = \text{rate (units/sec)} * \text{worth (\text{¢}/\text{unit})} * (0.7\% \Delta k/k/100\text{¢})$$
- 8. Document any relevant notes, comments, or observations on Attachment 5 data sheet.

Date of Change:
Change Approval
NETL Director

Stamp (Original-Red, Copy-Blue)

COPY

1



2
3

Reactivity vs. Power Ratio

Stamp(Original-Red, Copy-Blue)

Date of Change

NETL Director Approval

COPY

1
2
3
4

Rod: _____

$$P(\tau) = P_0 e^{\tau/T}$$

Date: _____

$$T = \Delta\tau / \ln(P(\tau)/P_0)$$

$$= \Delta\tau / \ln(10)$$

$$= .434 \Delta\tau$$

	Steady-state: ~3 watts				Rod positions		Times at power			
	TR	S1	S2	Reg	start	stop	60 watts	90 watts	600 watts	900 watts
1										
2										
3										
4										
5										
6										
7										
8										
9										
10										
11										
12										
13										
14										
15										
16										
17										
18										
19										
20										

5

Positive Period Data

Stamp(Original-Red, Copy-Blue)

Date of Change

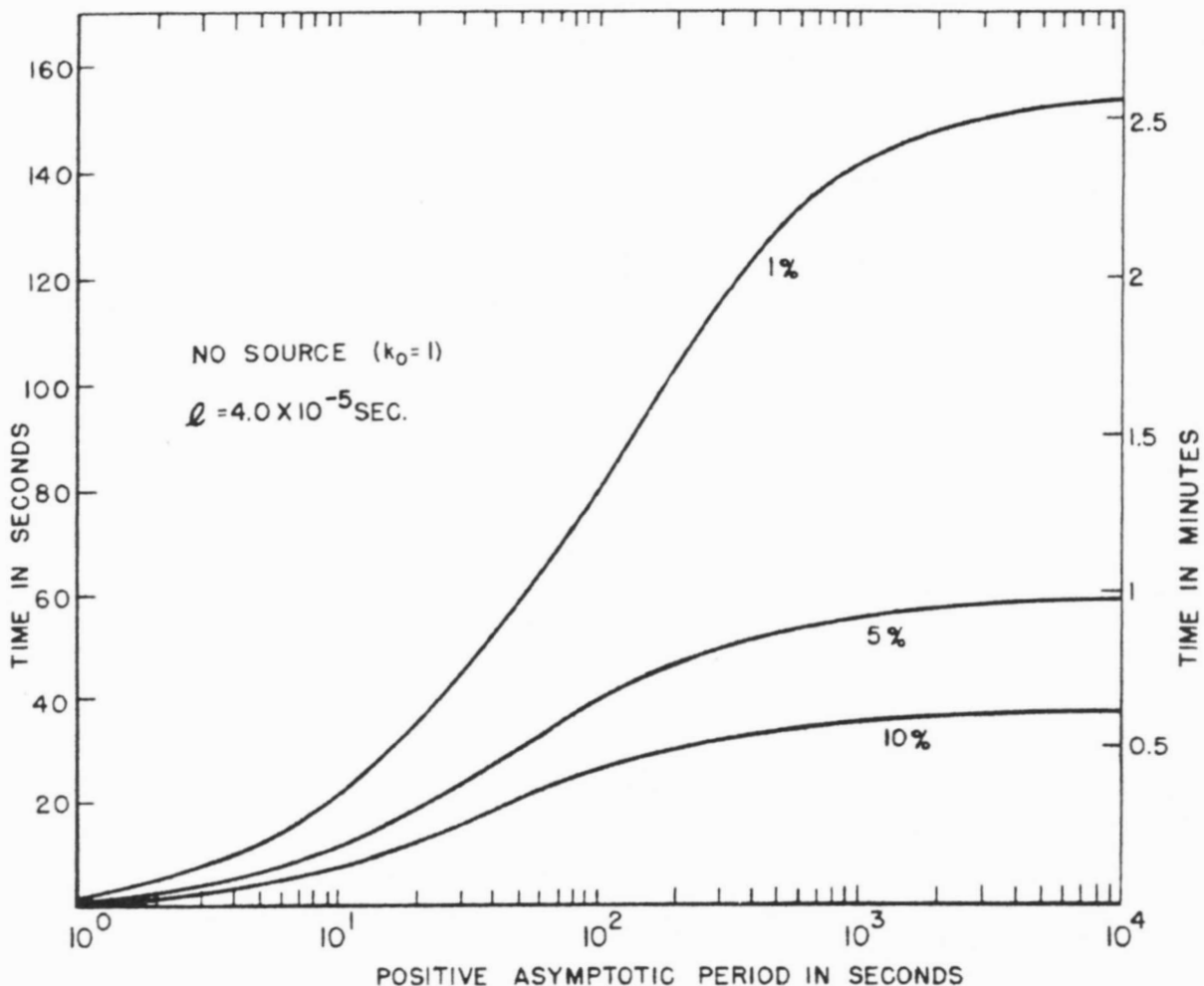
--	--	--	--	--

NETL Director Approval

--	--	--	--	--

COPY

1



2
3

Stable Period Wait Time

Stamp(Original-Red, Copy-Blue)

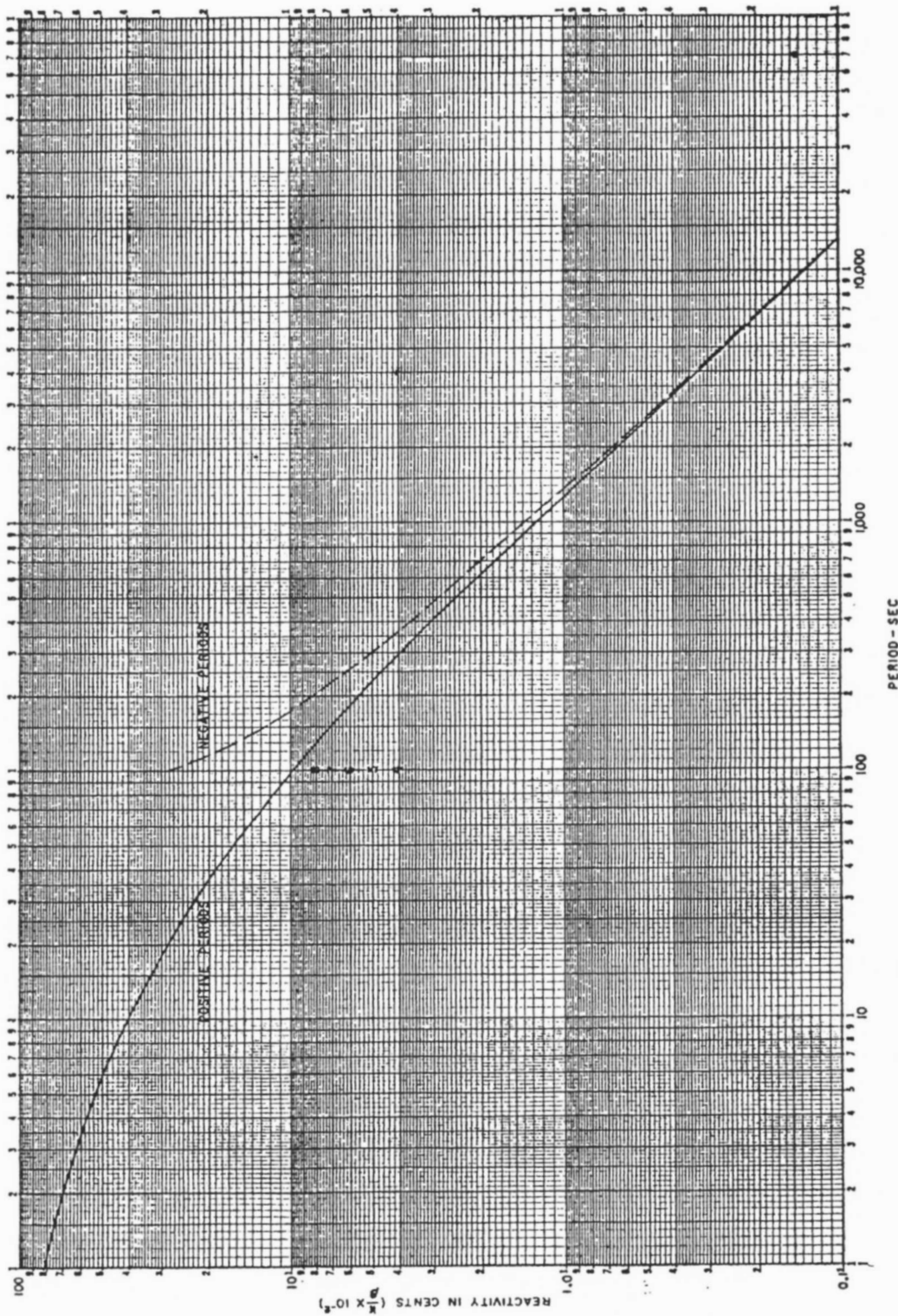
Date of Change

--	--	--	--

NETL Director Approval

--	--	--	--

COPY



Inhour Curve

Stamp(Original-Red, Copy-Blue)

Date of Change

--	--	--	--

NETL Director Approval

--	--	--	--

COPY

Rod Drop/Withdrawal Data

Rod Drop Time:

(limit: less than 1 second)

Rod	Time (Sec)	Verified OK (initial)
Transient		
Shim 1		
Shim 2		
Regulating		

Maximum Reactivity Insertion Rate:

(limit: less than 0.2 % ΔK/K/sec)

Rod	Withdrawal Time (sec)	Peak Differential Worth (¢/unit)	Insertion Rate (% ΔK/K/sec)
Transient			
Shim 1			
Shim 2			
Regulating			

Comments:

SRO Approval: _____ **Date:** ___/___/___

Rod Drop/Insertion Rate Data

Stamp(Original-Red, Copy-Blue)

Date of Change

--	--	--	--

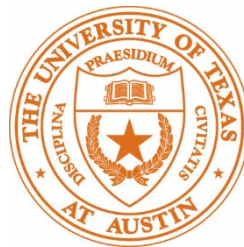
NETL Director Approval

--	--	--	--

COPY

**THERMAL HYDRAULIC ANALYSIS OF
THE UNIVERSITY OF TEXAS (UT) TRIGA REACTOR**

Paul (Michael) Whaley and William S. Charlton
Nuclear Engineering Teaching Laboratory
University of Texas at Austin
Austin, TX 78758



February 2023

1.0 Introduction

This report documents analysis of the thermal hydraulic characteristics of the UT TRIGA in support of renewal of the U.S. Nuclear Regulatory Commission facility operating license.

The UT-Austin TRIGA Research Reactor (UT TRIGA) is a TRIGA Mark-II nuclear research reactor licensed to The University of Texas at Austin for operation up to 1.1 MW steady-state thermal power level. The geometry of the UT TRIGA core is based on seven concentric hexagons (designated as rings) that fix locations for fuel elements, graphite filled elements, and various experiment facilities. The core is surrounded by a modified cylindrical annulus in an aluminum container filled with graphite (neutron reflector), a rotary specimen rack (RSR), four beam port penetrations, and void spaces accommodating the RSR and beam port facilities. The core and reflector are located in an aluminum tank (pool) filled with high-purity water. The water acts as a neutron moderator, coolant, and radiation shield.

Thermal hydraulic modeling of the UT TRIGA was performed with TRAC/RELAP Advanced Computational Engine (TRACE). Thermal hydraulic characteristics were developed from classical methods and corrections for UT TRIGA geometry using the computational fluid dynamics code FLUENT. Distribution of fission activity was developed from transport calculations in MCNP.

The thermal hydraulic codes TRACE and RELAP are designed to perform best-estimate analyses of operational transients and accident scenarios by modeling physical geometry and thermodynamic conditions. TRACE and RELAP were developed for commercial nuclear reactor applications, and RELAP has been widely used in characterizing research reactor thermal hydraulic performance. TRACE is the NRC's flagship thermal-hydraulics analysis tool consolidating and extending the capabilities of NRC's 3 legacy safety codes: TRAC-P, TRAC-B and RELAP.

NRC guidance¹ defines a "limiting core configuration" (LCC) as the core that would yield the highest power density using the fuel specified for the reactor, with all other core configurations demonstrated to be encompassed by safety analysis for the limiting core configuration. In this report, hot channel analysis was used to determine the power level and thermal hydraulic characteristics of the fuel element generating the highest power.

The guidance references an "operational core." Analytical methods used to define the LCC were applied to the operational core, providing confidence that the model adequately supports LCC analysis.

2.0 General Description of Heat Transfer at the UT TRIGA

Heat is generated in the fuel by the fission process. Cooling is required to maintain fuel temperature low enough to prevent challenges to cladding integrity. Fuel cladding is the principal safety feature of the TRIGA reactor, preventing radioactive fission products from release that could result in possible hazardous exposure to radiation for facility personnel and the general public. The UT TRIGA reactor operates in a natural convection-cooling mode. Heat transfer from fuel to the coolant in the core area is developed by generation of heat in the fission process, conduction of the heat to external surface of the fuel element, and heat transfer by convection from the fuel element surface to water in the core area.

Temperature increase of the water in the core area develops buoyancy forces that drive flow. The flow is diminished by momentum changes and friction (across the grid plates, fuel element end fittings, and fuel

¹ NUREG 1537, Guidelines for Preparing and Reviewing Applications for the Licensing of Non-Power Reactors, Format and Content

element cladding surfaces). Above a “critical” heat flux, coolant flow will not be adequate to prevent thermal hydraulic conditions from exceeding limits. This analysis demonstrates that operation at the maximum licensed power level has adequate margin to the fuel temperature limits and critical heat flux.

3.0 Power Distribution

The distribution of heat generation across the fuel elements in the core and the ratio of peak-to-average power in the hot channel fuel element (i.e., the fuel element producing the most power) are described in the Neutronics Report². The ratio of the hot channel peak power to element average power was derived from MCNP calculations for a 2-dimensional (axial and radial) mesh tally. Mesh tally results were used to develop power distribution profiles for a fuel element to support TRACE calculations.

4.0. Thermal Hydraulic Modeling, Unit Cell Geometry and Thermal Hydraulic Characteristics

4.1 UT-TRIGA Unit Cell Geometry

The flow channel unit cell cross section is based on the typical fuel element geometry, as illustrated in Fig. 4.1 (unit cell and the surrounding fuel elements). Some unit cell locations in the grid plate have different structures. The central thimble is not fueled, the transient rod does not contain fuel, and the fuel followers (which are generally not fully inserted in the core) have 80% of the fuel mass contained in standard fuel elements (which are generally not fully inserted). This analysis uses the hot channel identified in the neutronics report and assumes no interaction between adjacent unit cells. Any interaction between unit cells with fuel and adjacent unit cells with less or no fuel contributes a larger area where convection flow is the result of heat transfer from the fully fueled cell, resulting in enhanced heat removal from the fully fueled cell. Thus, from this standpoint the analysis here is conservative. As illustrated, the unit cell analysis is based on a fuel element and the surrounding flow area (end fittings have more complex geometry) circumscribed by a hexagon with an inner radius of $\frac{1}{2}$ of the pin-to-pin pitch. The complex geometries of the fuel element end fittings are approximated as hydrodynamic characteristics.

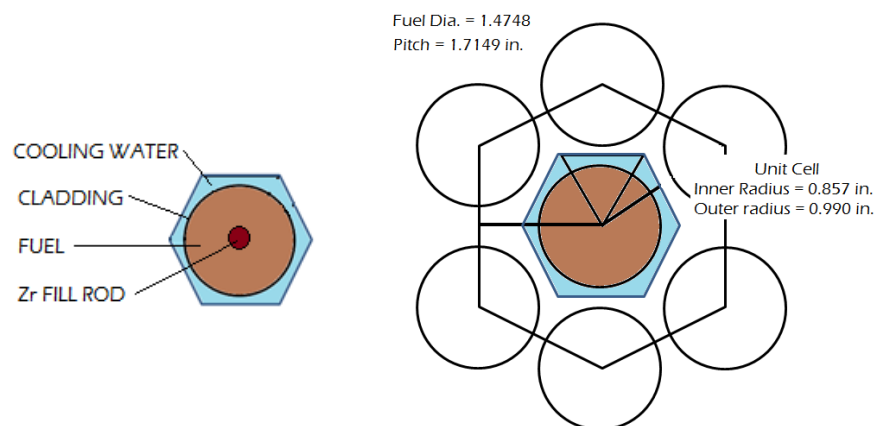


Figure 4.1, Flow Channel for UT TRIGA Fuel Elements

² Analysis of the Neutronic Behavior of the Nuclear Engineering Teaching Laboratory at The University of Texas, Radiation Center – Oregon State University (March 2021), submitted concurrently with this report

Since a regular hexagon can be decomposed into six equilateral triangles, a triangular unit cell is the smallest possible unit cell. However, TRACE heat structures (described in a following section) have limited options for temperature analysis of solid structures; a cylinder can be used to develop a fully symmetric heat source, but this is not possible with a half-cylinder. This does not limit fluid analysis in thermal hydraulic calculations with a triangular unit cell but limits the ability to calculate temperatures in the fuel element since the geometry of a triangular unit is ½ of the heat contribution from a single fuel element. Intrinsic properties used to calculate thermal hydraulic conditions are fully represented, but total heat for the cylindrical fuel element (used in material temperature calculations) in a triangular unit cell is not.

The volume of the flow channel is calculated as the product of the flow area and length. The length of the TRIGA flow channel is defined for the heated (adjacent to fuel) and unheated surfaces of fuel element cladding. The heated length is divided into smaller sections for analysis. The geometries and thermal hydraulic parameters of the upper and lower grid plate/fuel element are calculated through equations 4.1-4.9, with results summarized in Table 4.2.

The area of a regular polygon is calculated using the interior radius (r_i) and perimeter (P) as:

$$A = \frac{1}{2} \cdot r_i \cdot P \quad 4.1$$

The unit cell is a hexagon (i.e., 6-sided perimeter) with each side one leg of an equilateral triangle; the height of the triangle is the hexagon's interior radius. The hexagon/triangle dimension (a) in terms of the internal radius is calculated:

$$a = \frac{2}{\sqrt{3}} \cdot r_i \quad 4.2$$

Substituting 4.1 into 4.2, the cross-sectional area of the hexagonal unit cell (A_{UC}) using the interior radius is therefore:

$$A_{UC} = \frac{1}{2} \cdot r_i \cdot \left(6 \cdot \frac{2}{\sqrt{3}} \cdot r_i \right) = 2 \cdot \sqrt{3} \cdot r_i^2 \quad 4.3$$

The inner radius of the unit cell is ½ the distance between two fuel elements or ½ of the fuel element pitch (p_e) so that:

$$A_{UC} = \frac{\sqrt{3}}{2} \cdot p_e^2 \quad 4.4$$

The cross-sectional area of a fuel element (A_F) is calculated:

$$A_F = \pi \cdot \left(\frac{D_F}{2} \right)^2 \quad 4.5$$

The area of the flow channel in the unit cell (A_{FC}) is the difference between the unit cell area (eq. 4.1) and the area occupied by fuel (eq. 4.2). Since the interior radius is ½ of the pitch, the area of the flow channel is calculated by:

$$A_{FC} = \frac{\sqrt{3}}{2} \cdot p_e^2 - \pi \cdot \left(\frac{D_F}{2} \right)^2 \quad 4.6$$

The wetted perimeter is the length of the flow channel in contact with channel wall surfaces (i.e., the perimeter of the fuel element):

$$P_W = \pi \cdot D_F \quad 4.7$$

Non-circular pipes are approximated as a pipe with an equivalent hydraulic diameter (D_h) with a wetted perimeter (P_W), where the hydraulic diameter is calculated as:

$$D_h = \frac{4 \cdot A_{FC}}{P_W} \quad 4.8$$

Substituting equations 4.6 and 4.7 for flow area and perimeter into equation 4.8, the hydraulic diameter is given by:

$$D_h = \frac{4}{\pi \cdot D_F} \cdot \left[\frac{\sqrt{3}}{2} \cdot p_e^2 - \pi \cdot \left(\frac{D_F}{2} \right)^2 \right] = \frac{2 \cdot \sqrt{3}}{\pi} \cdot \frac{p_e^2}{D_F} - D_F = D_F \cdot \left[\frac{\sqrt{3}}{2} \cdot \frac{p_e^2}{D_F^2} - 1 \right] \quad 4.9$$

A summary of primary and calculated parameters using the equations above is provided in Table 4.1.

Table 4.1, Summary of Principle Thermal Hydraulic Values

Description	Var.	Value							
Fuel Element Pitch	P	1.7149	in	0.1428	ft	4.3535	cm	0.04353	m
Fuel Element Diameter	D_{fuel}	1.4784	in	0.1232	ft	3.7551	cm	0.03755	m
Wetted Perimeter	P_W	4.6445	in	0.3870	ft	11.7971	cm	0.1179	m
Fuel Cross Section/Area	A_{FC}	1.7166	in ²	0.01192	ft ²	11.0749	cm ²	0.001107	m ²
Unit Cell Area	A_{Cell}	2.5442	in ²	0.01766	ft ²	16.4142	cm ²	0.001641	m ²
Flow Channel Area	A_{FC}	0.8275	in ²	0.005747	ft ²	5.3392	cm ²	0.000534	m ²
Hydraulic Diameter	D_h	0.7127	in.	0.05939	ft.	1.8103	cm	0.01810	m

4.2 UT TRIGA Thermal Hydraulic Model

TRACE analysis is based on modeling a set of representative TRACE components with characteristics specified by the user to model the system. The UT TRIGA model uses Break, Pipe, Heat Structure, and Power components. These TRACE components were assembled as shown in Fig. 4.2 to model the thermal hydraulic performance of the unit cell flow channel.

4.2.1 Break:

A break is a boundary component normally used as a sink for liquid flows exiting the system³, here simulating pool water entering and exiting the flow channel. Break pressure and temperature specifications are based on local environmental conditions (barometric pressure, confinement control), pool level, and water temperature. Pressure boundary conditions for limiting and nominal cases are provided in Table 4.2. UT TRIGA flow is calculated by TRACE as developed by convection in reactor operation.

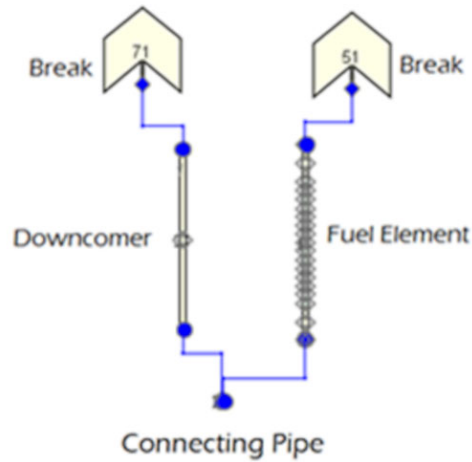


Figure 4.2, TRACE Model

The NETL building is approximately 240 m above sea level, corresponding to 96 kPa at standard atmospheric conditions. The reactor bay confinement system is designed to control differential pressure to 0.06 in. (14.9 Pa) below atmospheric (minimal compared to atmospheric pressure). Total pressure at the top of the core is therefore:

$$p_T = 96 \{KPa\} + p_{H_2O} \quad 4.10$$

Pool water is a minimum of 5.25 m above the core, nominally 7.25 m. Constant pressure is established by setting the “rate of change” variable to zero in the break, and with a single value for pressure over RELAP time intervals. Pool water temperature is limited to less than 49 °C, nominally 25-27 °C. Where g denotes the gravitational constant ($9.8 \text{ m}\cdot\text{s}^{-2}$), the pressure (p_{H_2O}) exerted by a column of water (at density ρ in $\text{kg}\cdot\text{m}^{-3}$ and height h in m) is given by:

$$p_{H_2O} = \rho \cdot g \cdot h \quad 4.11$$

Table 4.2, Pressure Boundary Condition

Condition	Temperature °C	Density $\text{kg}\cdot\text{m}^{-3}$	Height m	Hydrostatic Pressure kPa	Pressure kPa	Pressure Psia
Limiting	49	988.4881	5.25	50.9	146.9	21.3
Nominal	25	997.0479	7.25	70.8	166.8	24.2
	27	996.5162	7.25	70.8	166.8	24.2

³ TRACE has a Fill component, but Break component calculates flow rate while Fill requires specifying a flow rate.

4.2.2 Pipe

The pipe component is a cylindrical volume for water flow with user-specified geometric and hydrodynamic properties. One pipe (downcomer) represents movement of cooling flow from the inlet break to the bottom of the flow channel. A second pipe (connector) moves flow to the entrance of the flow channel and connects the down comer to the third pipe (unit cell flow channel). The third pipe discharges to the outlet break.

4.2.3 Down-comer/Cold Leg

Conservation requirements for calculations require balanced elevation changes, with a “downcomer” at the same length and area as the fuel element region. Instabilities can occur in TRACE calculations if adjacent volumes are sufficiently different, and the downcomer is segmented to meet the ratio criteria (for convenience, segmenting has equal lengths). Dimensions for the downcomer pipe are provided in Table 4.3. The direction of flow is down.

Table 4.3, Downcomer Pipe

Length (segments)	0.09985 m
Length (total)	0.5991 m
Flow area	5.39E-4 m ²
Volume (segments)	5.38E-5 m ³
Volume (total)	3.23E-4 m ³
Hydraulic diameter	0.0183 m
Height Change (segments)	-0.09985 m
Height Change (total)	-0.5991 m

4.2.4 Connector

A pipe with two elbows (Fig. 4.3) connects flow from the downcomer to the unit cell flow channel. Dimensions of the connecting pipe are provided in Table 4.4. Inlet flow is down, outlet flow is up, and the intermediate flow is horizontal.

Table 4.4, Connecting Pipe

Segment	Volume m ³	Length m	Flow Area m ²	Height Change M
1	5.38E-05	0.01	5.39E-04	-5.0E-3
2	5.38E-05	0.01	5.39E-04	0.0
3	5.38E-05	0.01	5.39E-04	5.0E-3

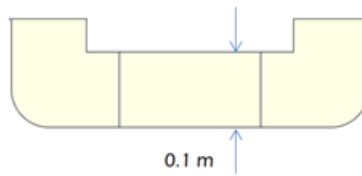


Figure 4.3, Cold Leg to Flow Channel Connector

4.2.5 Unit Cell Flow Channel/Fuel Element Region

The flow channel for the fuel element region in the unit cell is modeled as a pipe with heated lengths connected to a heat structure. Specifications for the simulated fuel element cooling channel are provided in Table 4.5. The K factors are applied to the 2nd and the 19th segments. Flow is up. Traditional K factors are discussed, followed by development of UT TRIGA specific K factors.

Table 4.5, Specifications for Unit Cell Flow Channel

Segment	Volume m ³	Length m	Flow Area m ²	Δz M
1	5.14E-06	0.01905	2.70E-04	0.01905
2	2.43E-05	0.09	2.70E-04	0.09
3	6.86E-06	0.0254	2.70E-04	0.0254
4	6.86E-06	0.0254	2.70E-04	0.0254
5	6.86E-06	0.0254	2.70E-04	0.0254
6	6.86E-06	0.0254	2.70E-04	0.0254
7	6.86E-06	0.0254	2.70E-04	0.0254
8	6.86E-06	0.0254	2.70E-04	0.0254
9	6.86E-06	0.0254	2.70E-04	0.0254
10	6.86E-06	0.0254	2.70E-04	0.0254
11	6.86E-06	0.0254	2.70E-04	0.0254
12	6.86E-06	0.0254	2.70E-04	0.0254
13	6.86E-06	0.0254	2.70E-04	0.0254
14	6.86E-06	0.0254	2.70E-04	0.0254
15	6.86E-06	0.0254	2.70E-04	0.0254
16	6.86E-06	0.0254	2.70E-04	0.0254
17	6.86E-06	0.0254	2.70E-04	0.0254
18	2.43E-05	0.09	2.70E-04	0.09
19	5.14E-06	0.01905	2.70E-04	0.01905
Total	1.62E-04	0.5991	5.13E-03	0.5991

4.2.6 Headloss (K) factors

Pressure drops (head loss) across hydraulic components are the product of the fluid flow and factors such as the coefficient of friction between the fluid and the pipe wall, changes in flow area and diameter, flow channel surface roughness, and/or flow channel length. Within limits, the factors (K factors) are constant, the sum of the pressure drops in linear flow is additive. This analysis provides a traditional approach to evaluating the loss factors and loss factors reported by analysis and

experiments conducted at the UT reactor, followed by the results of analysis and experiments conducted specific to the UTRIGA facility.

4.2.7 Classic K factors

The impact of sudden expansion or contraction is principally in velocity changes. Traditional K factors for sudden expansions or contractions are based on the ratio of inlet and outlet flow areas (Table 4.6, Equation 4.12).

$$K_e = \left[1 - \frac{d_1^2}{d_2^2} \right] = \left[1 - \frac{A_1}{A_2} \right] \quad 4.12$$

Other K factors are based on the magnitude of the direction change, the pipe surface roughness, and flow mode (turbulent, laminar, etc.). Calculations are simplified by using the Darcy-Weisback friction factor (f) as a multiplier on applicable aspects of system geometry. The friction factor is a function of the Reynolds number, wall surface roughness, and flow channel. The relationship is described in the Colebrook formula:

$$\frac{1}{\sqrt{f}} = -2.0 \cdot \log_{10} \left(\frac{\varepsilon}{3.7 \cdot D} + \frac{2.51}{\text{Re} \cdot \sqrt{f}} \right) \quad 4.13$$

In practice, the Moody chart is frequently used to determine the friction factor. For reasonable and expected flow rates at the TRIGA reactor, the Reynolds number is between 1×10^4 and 3×10^5 . Over this range, convergence exists for wall surface roughness values between 5×10^{-7} to 1×10^{-3} . The broad range of surface roughness values indicates a very low sensitivity for roughness, and that any surface roughness within this range can be used without affecting the friction factor significantly. For comparison, RELAP analysis conducted for DOW Chemical⁴ reactor used surface roughness of 2.13×10^{-6} .

For losses in a straight pipe:

$$K = f \cdot \frac{L}{D} \quad 4.14$$

For a 45° turn:

$$K_{45} = f \cdot 16 \quad 4.15$$

For a 90° turn:

$$K_{90} = f \cdot 30 \quad 4.16$$

Table 4.6:

Location	Component	Eff. Area
Bottom Entrance	Lower grid plate	1.2 cm ²
Bottom Exit	Lower End fitting/Channel	3.9 cm ²
Top Entrance	Upper End Fitting/ Channel	3.9 cm ²
Top Exit	Upper Grid Plate	1.2 cm ²

⁴ ANALYSIS OF THE THERMAL HYDRAULIC AND REACTIVITY INSERTION BEHAVIOR OF THE DOW TRIGA RESEARCH REACTOR, Submitted to the NRC in support of the DTRR License Renewal (M. H. Hartman, 03/12/2011).

The K factor for elevations above the flow channel is based on a 45° turn out of the main channel and sudden contraction at the upper grid plate. The K factor below the flow channel is based on a sudden expansion exiting the grid plate and a 45° turn into the main channel.

4.2.8 UT TRIGA Specific K factors

Correlation of K factors to flow are based on historical, experimental measurements with cylindrical pipes, with additional work validating this approach for rectangular ducts. In practice, non-circular cross sections are reduced to a flow area and a hydraulic diameter, with length as measured for the pipe. However, the complexity of the TRIGA inlet and exit flow channel geometry is challenging. As fluid interacts with non-circular structures (or components), non-uniform surfaces can result in forces leading to secondary and/or internal flow paths that affect head loss/pressure drops. This suggests two potential issues using K factors calculated classically in analyzing thermal hydraulic response of the TRIGA reactor:

- The actual entrance and exit to the flow channel between the grid plates is directed by fins mounted on a conical shape that terminates in cylindrical alignment (bottom end fitting) and handling (upper end fitting) structures. The wetted perimeters and flow areas vary continuously from entrance and exit for each end fitting.
- The interface between adjacent fuel channels is not separated by a physical boundary. Differential pressure between adjacent flow channels at interfaces can support cross-channel flow.

Therefore, thermal hydraulic analysis to support relicensing was developed⁵ to:

- (1) Model the UT TRIGA reactor using TRACE
- (2) Develop an independent solution tool using MATLAB to calculate thermal hydraulic performance based on mass and energy balance and K factors,
- (3) Develop a computational fluid dynamics model using FLUENT, and
- (4) Conduct experiments to develop a UT TRIGA specific heat transfer correlation.

These methodologies were used to independently model thermal hydraulic performance from (1) first principles, (2) TRACE thermal hydraulics code, and (3) FLUENT computational fluid dynamics code. The results of experiments in the TRIGA core were used to evaluate UT TRIGA-specific K factors based on actual fuel element geometry. A summary of K values determined from both the traditional/classical method and the UT FLUENT analysis is provided in Table 4.7, with a fractional deviation between factors provided. For comparison, RELAP work⁶ performed for DOW Chemical facility used K factors of 2.26 and 0.63 for the lower and upper channels respectively. The values determined from the UT FLUENT analysis were used in modeling for TRACE calculations.

Table 4.7, K Factors

⁵ Development of Thermal Hydraulic Correlations for the University of Texas at Austin TRIGA Reactor Using Computational Fluid Dynamics and In-Core Measurements, A. D. Brand

⁶ ANALYSIS OF THE THERMAL HYDRAULIC AND REACTIVITY INSERTION BEHAVIOR OF THE DOW TRIGA RESEARCH REACTOR, Submitted to the NRC in support of the DTRR License Renewal (M. H. Hartman, 03/12/2011).

APPLICATION	CLASSICAL	FLUENT ⁷	DEVIATION
Lower Channel	1.244	1.63	23.7%
Upper Channel	0.844	1.12	33.6%

4.2.9 Heat Structure

TRACE defines heat structures as rigid components that absorb, transfer, or radiate heat. The heat structure is specified by geometry, inner and outer radial boundary conditions, and material information. Boundary conditions for heat transfer are specified for axial nodes/surfaces, linking the heat source to the heated lengths of the pipe to represent the active (fueled) part of the fuel element. Heat structure cells simulate the zirconium fill rod at the center of the fuel element, ZrH-U fuel, the gap between the fuel and cladding, and the cladding. Heat structure material properties are used to calculate temperature distribution for fuel element components (zirconium fill rod, U-ZrH matrix, gas gap, and cladding). The material in the UT TRIGA model includes:

- Zirconium from a radius of 0 cm to 0.3175 cm (3.175E-3 m)
- Zirconium-hydride from a radius of 0.3175 cm to 1.74117 cm (0.0174117 m), subdivided into 15 segments, 13 equal volume segments with one segment boundary at thermocouple location
- Gap gases from a radius of 1.74117 cm to 1.8161 cm (0.018161 m)
- Stainless steel 304 cladding from a radius of 1.8161 cm to 1.8671 cm (0.018671 m)

The effects of core reactivity on the hot channel are simulated by defining a heat structure for the flow channel. When this option is selected it is necessary to set initial conditions for the average fuel element and implement the hot channel power peaking factor from the Neutronics Analysis.

4.2.10 Gas-Gap Heat Transfer Coefficient

There is a small difference in the outer radius of the fuel element matrix and the inner radius of the fuel element cladding. This annulus contains hydrogen and fission product gases in a balance between evolution from and reabsorption into fuel matrix. The heat transfer coefficient (HTC) of the gap is a complicated function of geometry, surface roughness at solid to gaseous interfaces, differential pressure, and constituent gas properties⁸, all of which are variable with temperature and unknown. Correlations for power reactors are built into TRACE, but for applications other than power reactors only a single HTC value can be used in a calculation.

The UT TRIGA reactor has two fuel elements instrumented with thermocouples that monitor fuel temperature in positions that produce power levels at or near the hot channel power. The construction of the instrumented elements varies from standard fuel elements with (small) channels for thermocouple leads and (small) penetrations for the thermocouples. The instrumented elements are designed to be representative of standard fuel elements for initiation of protective action. The fuel mass is roughly 97% of the mass of a standard fuel element, and the gap geometry of the instrumented element is therefore similar to the gap of standard fuel elements.

⁸ Elements of Nuclear Reactor Design, 2nd Edition (J. Weisman) & TRACE V5 Theory Manual, pages 438-441

4.2.11 Power Component

The power component includes fundamental nuclear data such as fissile isotope Q values and fission fractions, delayed neutron data, decay heat model, power distribution, reactivity coefficients, and time-based profiles for power or reactivity in transient problems. The ANSI/ANS-5.1-2014 standard (Decay Heat Power in Light Water Reactors) was used as the decay heat model.

Nuclear data was provided by the MCNP calculations in the Neutronics Report. The ratio of decay heat power to initial reactor power depends on a reactor specific energy generation per fission (MeV/fission) used in TRACE transient calculations. The TRACE point reactor kinetics treatment uses fission product nuclear characteristics (precursor fractions, decay constants, and the generation time) from MCNP adjoint calculations for the current core configuration (i.e., in validation) and the LCC. The MCNP burnup analysis output supporting the Neutronics Report tabulates fission energy yield data (Q value) as given in Table 4.8.

Table 4.8: Fission Energy Yield from MCNP Analysis

Nuclide	Q-Value (MeV)
92235	180.99
92238	181.31
94239	189.44
94241	189.99

The fraction of energy produced by each fissionable material (Table 4.9) for TRACE analysis is taken from the MCNP burnup calculations. The estimate of the fraction of isotope 92235 fissions at greater than thermal energy is assumed to have a Q value consistent with isotope 92238.

Table 4.9: Fission Isotope Nuclear Characteristics⁹

Nuclide	Fraction	Fission Cross-section (b)	Energy Range	Fissions at Energy
92235	19.8%	585.1	<0.625 eV	94.28%
		274.4	0.625 ev – 100 kev	4.99%
92238	80.2%	1.241	>100 kev	0.72%
		0.03064		

MCNP adjoint calculations provided estimates of the prompt neutron generation time and effective delayed neutron fractions. The prompt-neutron generation time was reported as $43.81 \pm 0.53 \mu\text{s}$. The 1992 Safety Analysis Report for the UT TRIGA cited a prompt generation time of $41 \mu\text{s}$, which is reasonably consistent with that calculated by MCNP. The MCNP calculated value utilizing current parameters is used in this report.

An MCNP calculation incorporating the KOPTS option was used to provide delayed neutron precursor data (Table 4.10) for the current core described in the Neutronics report.

Table 4.10: Nominal Core Delayed Neutron Precursor Group Characteristics

⁹ <https://www.ndc.jaea.go.jp>; Fission at Energy from MCNP burnup calculation

Group	β_i	Standard Deviation	Energy (MeV)	Standard Deviation	λ_i (s ⁻¹)	Standard Deviation	$T_{1/2}$ (s)
1	0.00024	0.00004	0.41037	0.00353	0.01334	0.00000	51.974
2	0.00117	0.00009	0.47158	0.00158	0.03271	0.00000	21.189
3	0.00098	0.00007	0.44336	0.00159	0.12074	0.00000	5.741
4	0.00287	0.00013	0.55738	0.00142	0.30288	0.00001	2.288
5	0.00116	0.00009	0.51857	0.00230	0.85033	0.00003	0.815
6	0.00047	0.00006	0.54495	0.00392	2.85505	0.00020	0.232

The time dependent behavior of power following shutdown was evaluated and developed using reactor kinetics for fission power and the method of ANSI/ANS-5.1-2014 (equations 7 and 8) for decay heat from fission products. For an irradiation interval of time T , a decay time of t , and irradiation intervals i and a constant fission rate of unity, decay heat power (F , units of MeV/fission) is represented analytically as a function (equation 4.17) using analytic fit constants α and β (provided for all 23 components in the standard):

$$F_I(t, T_a) = \sum_{j=1}^{23} \frac{\alpha_{i,j}}{\lambda_{i,j}} \cdot \exp(-\lambda_{i,j} \cdot t) \cdot [1 - \lambda_{i,j} \cdot T] \quad 4.17$$

Assuming a single continuous power generation interval and a long operating time, equation 4.17 reduces to equation 4.18:

$$F_I(t) = \sum_{j=1}^{23} \frac{\alpha_j}{\lambda_j} \cdot \exp(-\lambda_j \cdot t) \quad 4.18$$

Power distribution based on the results of the Neutronics Report MCNP model and power distribution in TRACE is implemented as the fraction of power generated between the inner and outer radial boundaries at each axial node. The power distribution in the UT TRACE model is a 2 dimensional, radial and axial, distribution based on the Neutronics Report MCNP model.

Steady state calculations were performed to establish operational characteristics for evaluating the critical heat flux ratio and also to provide initial conditions for some transient calculations. Transient power calculations were performed to establish initial conditions for loss of cooling analysis. Transient reactivity calculations were performed for pulsing from low power, pulsing from power above the point of sensible heat production, continuous reactivity additions, and a fuel element discharged from the core and air cooled.

4.2.12 Materials

TRACE has a limited set of material characteristics applicable to nuclear power plants, with only gap gases and stainless steel 304 applicable to TRIGA reactors. The default set of materials were user-augmented with zirconium and uranium zirconium. User defined materials are defined in a data table specified over a range of temperature, and include (1) density, (2) specific heat capacity, (3) thermal conductivity, and (4) emissivity.

The thermal conductivity of TRIGA fuel is noted to be $0.042 \text{ cal}\cdot\text{s}^{-1}\cdot\text{cm}^{-1}\cdot\text{°C}^{-1}$ ($17.573 \text{ W}\cdot\text{m}^{-1}\cdot\text{°K}^{-1}$)¹⁰, and is assumed to be insensitive to temperature. The volumetric heat capacity (C_v , referenced to temperature T in °C) was calculated using:

$$C_v = 2.04 + 4.17 \times 10^{-3} \cdot T \left\{ \frac{\text{W} \cdot \text{s}}{\text{cm}^3 \cdot \text{°C}} \right\} \quad 4.19$$

Specific heat capacity is calculated by normalizing the volumetric heat capacity to density (ρ), with the density of the fuel matrix. The density of ZrH for hydrogen to zirconium ratio (R) of 1.6 or greater is given by:

$$\rho_{\text{ZrH}} \left\{ \frac{\text{g}}{\text{cm}^3} \right\} = \frac{1}{0.1706 + 0.0042 \cdot R} \quad 4.20$$

The uranium density is 19.07 g/cm^3 . The weight per cent for the two components is indicated by subscripts, U for Uranium ZrH for Zirconium-Hydride so that the fuel matrix density is:

$$\rho_{U-ZrH,1.6} \left\{ \frac{\text{g}}{\text{cm}^3} \right\} = \frac{1}{\frac{w_U}{\rho_U} + \frac{w_{ZrH}}{\rho_{ZrH}}} \quad 4.21$$

Since the fuel heat capacity is a linear function with respect to temperature, only two values that bound the calculations were used (Table 4.8).

Thermal conductivity for the zirconium fill rod at the center of the fuel element was taken (even 100 temperature values) from the *Journal of Physical and Chemical reference Data (Volume 3, 1974, Supplement 1, Table 184)*, with intermittent values interpolated. Volumetric heat capacity data was taken from a compilation¹¹, with data interpolated by a curve fit. Mass-specific heat capacity used in TRACE is calculated as the ratio of the volumetric heat capacity to the density. Zirconium and uranium-zirconium-hydride data is provided in Table 4.11.

Table 4.11, User Supplied Material Data

Material	T °K	P kg·m ⁻³	C _p W·s·kg ⁻¹ ·K ⁻¹	Conductivity W·m ⁻¹ ·K ⁻¹	Emissivity
Uranium-Zirconium-Hydride	293.15	5998.595	353.88	18.01	0.8
	3033.15	5998.595	3815.01	18.01	0.8
Zirconium	200.15	5256.94	344.276	25.19226	0.8
	400.15	5256.94	427.5999	21.59248	0.8
	600.15	5256.94	510.9237	20.68942	0.8
	800.15	5256.94	594.2475	21.59248	0.8
	1000.15	5256.94	677.5714	23.69131	0.8
	1200.15	5256.94	760.8952	25.98944	0.8
	1500.15	5256.94	885.881	28.78582	0.8
	2744.928	5256.94	1404.479	37.43582	0.8

¹⁰ Simnad, *The U-ZrHx Alloy: Its Properties and Use in TRIGA Fuel* (August 1980)

¹¹ <http://www.efunda.com>

4.2.13 Temperature Coefficients of Reactivity

The Fuel Temperature Coefficient of Reactivity (FTC) was developed from the Neutronics Report's MCNP model with cross-sections at temperatures taken from the distributed libraries for scattering data and isotopes for comparison to the FTC from General Atomics. There are 8 sets of scattering data and 4 sets of isotope cross sections corresponding to the scattering data within MCNP. Where scattering data at specific temperatures do not have corresponding scattering cross section data, an auxiliary program (MAKXSF) was used to develop interpolated cross sections at scattering data temperatures. Calculations using the fuel temperature data were performed at three water temperatures: nominal operating temperature, maximum permitted pool temperature, and a value approximately half-way between the two. The values for k_{eff} were fit to a curve (first varying the fuel temperature, then varying the moderator temperature), and the formulae used to generate data $\frac{1}{2}$ degree above and $\frac{1}{2}$ degree below the temperature of interest. The FTC, reactivity associated with a 1 degree change in temperature, was calculated as:

$$\frac{d\rho}{dT} = \frac{k_{eff,T+\frac{1}{2}} - k_{eff,T-\frac{1}{2}}}{k_{eff,T+\frac{1}{2}} \cdot k_{eff,T-\frac{1}{2}}} \quad 4.22$$

The moderator temperature coefficient was very small compared to the FTC, and the difference between the k_{eff} values at each moderator temperature was therefore not significant to the FTC. The MCNP-based FTC is shown in Figure 4.4. Also, shown in the figure is historical GA data. General Atomics¹² indicates that the fuel temperature coefficient (water reflected) is convex, with a minimum occurring about 300°C. The MCNP-based FTC for the UT TRIGA agrees well with the GA data above 200°C. At low temperatures the MCNP-based FTC deviates from the General Atomics FTC, but the general shapes are similar. The distribution of cross sections temperatures is too broad to reflect the changes when k_{eff} changes quickly with respect to temperature, which affects the FTC calculation. There is a decrease to a minimum value of FTC and then nearly a linear increase above the minimum FTC for both MCNP-based and the General Atomics provided data (Table 4.12 and Fig. 4.4). The moderator temperature coefficient (Table 4.13 and Fig. 4.5) was also developed from the MCNP data.

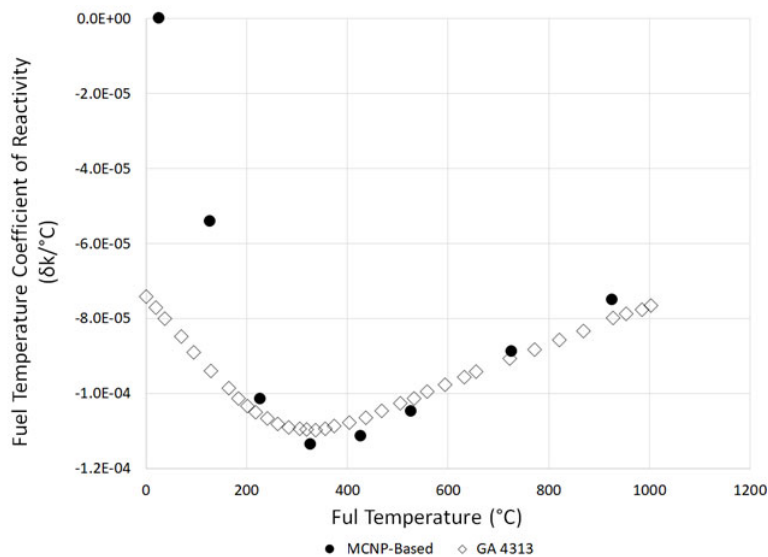


Figure 4.4: MCNP-Based FTC and GA FTC

¹² Simnad op. cit.

Table 4.12, MCNP-Based Fuel Temperature Coefficient

Fuel Temperature °C	FTC $\delta k/^\circ\text{C}$
26.85	-4.96E-08
126.85	-5.41E-05
226.85	-1.01E-04
326.85	-1.14E-04
426.85	-1.11E-04
526.85	-1.05E-04
726.85	-8.89E-05
926.85	-7.50E-05

Table 4.13, Moderator Temperature Coefficient ($\delta k/^\circ\text{C}$)

Fuel Temperature		24 °C	427 °C	927 °C
Moderator (Pool) Temperature	24 °C	-1.65E-0	-1.76E-5	-1.93E-5
	51 °C	-5.47E-0	-5.84E-6	-6.44E-6
	101 °C	1.75E-0	1.87E-5	2.05E-5

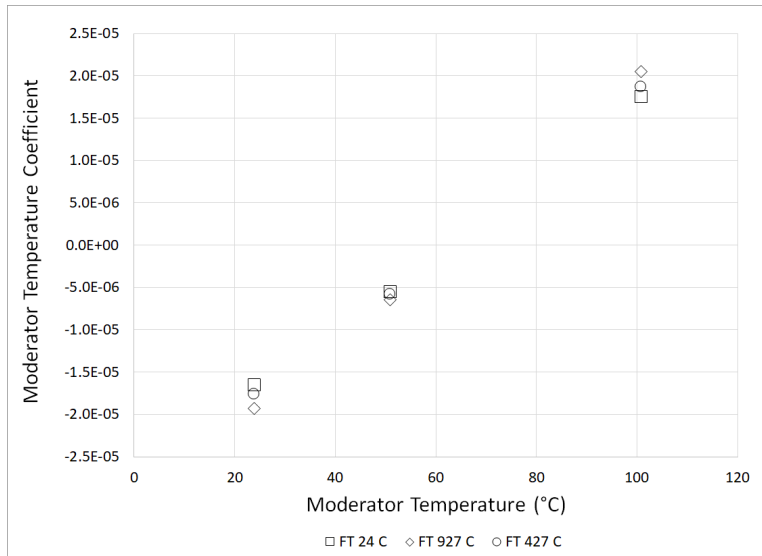


Figure 4.5: Moderator Temperature Coefficient

Analysis at AFRR1¹³, based on DIF3D (Argonne National Laboratory, diffusion, and transport theory code) shows convex fuel temperature reactivity structure from 10-1000°C for TRIGA fuel. Calculations based on DIF3D indicate fuel coefficient reactivity range from -8×10^{-5} to $-1.2 \times 10^{-4} \Delta k/k \text{ } ^\circ\text{C}^{-1}$ for a TRIGA core with a circular grid plate (the UT TRIGA has a hexagonal pitch). The values in Fig. 4.4 are in reasonable agreement with this analysis.

¹³ AFRR1 op. cit.

4.2.14 Critical Heat Flux Ratio

Critical heat flux ratio (CHFR) is the ratio of the critical heat flux (CHF) to the actual heat flux. ANL/RERTR/TM-07-01 provides a series of calculations with different correlations for critical heat flux, including the Bernath correlation. The correlation for critical heat flux developed by Bernath is recommended by the reference in evaluating TRIGA fuel performance. The Bernath correlation (where CHF_{BO} is the heat flux that results in burnout, h_{BO} is the convection heat transfer correlation at burnout, $T_{W,BO}$ is the temperature of the cladding surface at burnout, and V is the fluid velocity, T_b is the cooling water bulk temperature, and dimensional variables as described in Table 4.14) determines the critical heat flux that results in burnout as:

$$CHF_{BO} = h_{BO} \cdot (T_{W,BO} - T_b) \quad 4.23$$

where the heat transfer coefficient for burnout conditions is calculated using:

$$h_{BO} = 10890 \cdot \frac{D_e}{D_e + D_i} + V \cdot \frac{48}{D_e^{0.6}} \quad 4.24$$

The formula predicting wall temperature at burnout is:

$$T_{W,BO} = 57 \cdot \ln P - 54 \cdot \frac{P}{P+15} - \frac{V}{4} \quad 4.25$$

Substituting equations 4.23 and 4.24 into equation 4.25 results in:

$$CHF_{BO} = \left[10890 \cdot \frac{D_e}{D_e + D_i} + V \cdot \frac{48}{D_e^{0.6}} \right] \cdot \left(\left[57 \cdot \ln P - 54 \cdot \frac{P}{P+15} - \frac{V}{4} \right] - T_b \right) \quad 4.26$$

The Bernath formulation is in "pound centigrade units," converted to $\text{BTU h}^{-1} \text{ft}^{-2}$ by multiplying by a factor of 1.8:

$$W_{CHF} = 1.8 \cdot \left[10890 \cdot \frac{D_e}{D_e + D_i} + V \cdot \frac{48}{D_e^{0.6}} \right] \cdot \left(\left[57 \cdot \ln P - 54 \cdot \frac{P}{P+15} - \frac{V}{4} \right] - T_b \right) \quad 4.27$$

Table 4.14, Bernath Correlation Variables

Variable	Description	Units	Source
D_e	Hydraulic diameter	Ft	Previous formula
D_i	Heater surface diameter	Ft	Fuel element diameter ³
V	Pressure	Psia	Calculated by TRACE
P	Velocity	$\text{ft} \cdot \text{s}^{-1}$	Calculated by TRACE
T_B	Coolant Temperature	$^{\circ}\text{C}$	Calculated by TRACE

5.0 Model Validation

The model described above was validated by comparison of model results to measured parameters from the UT TRIGA reactor. Nominal values indicated in Table 5.1 are used in validation.

Table 5.1, Model Input Values

Description	Source or Value
Pressure and Temperature	Table 2.4
K-Factors (Fluent)	Table 4.7
Fission Energy Yields	Table 4.10
Thermal and Fast Fission Fractions	Table 4.11
Delayed Neutron Precursor Data	Table 4.12
User Supplied Material Data	Table 4.13
Fuel Temperature Coefficient	Table 4.14
Moderator Temperature Coefficient	Table 4.15
Prompt Neutron Generation Time	47 μ s ¹⁴
Core Radial Peaking Factor	1.68 ¹⁵
Wall Surface roughness	6.998032E-6

5.1 Operating Data

The Integrated Control System (ICS) reports peak power and peak temperature from a thermocouple in an Instrumented Fuel Element during normal and pulsing operations. Measured fuel temperature channel indications at varying power level are compared to thermocouple location temperatures calculated by TRACE. There is no actual measurement of heat fluxes available for comparison with calculations of critical heat flux ratio, CHF_R (the ratio of fuel element local heat flux to the heat flux that could result in departure from nucleate boiling). During pulsing, core peak power is reported. TRACE calculations of an average fuel element were compared to ICS data (peak power distributed over all elements in the core) and the TRACE calculated temperature at a location similar to the IFE thermocouple location is compared to ICS data.

5.2 Temperature Instrumentation

Instrumented fuel elements (IFEs) are located in the B ring. Three thermocouples are installed in each IFE, with one thermocouple in each IFE normally instrumented. The thermocouples are located 0.762 cm from the center of the fuel element, with one an inch above the mid-plane, a second at the mid-plane, and a third an inch below the mid-plane. TRACE calculations show the thermocouple response varies only slightly between the three elevations.

5.3 Steady-State Validation

The temperatures of the thermocouple locations used in the measuring channel were calculated using the TRACE model during steady-state operation. One thermocouple was replaced in February 2016. Consequently, the baseline temperature data for validation is taken from December 2015 through February 2016 with IFE load configurations as specified in Table 5.2.

The Neutronics Report was developed using an MCNP burn-card to generate an estimate of the material composition for each fuel element in the TRIGA core at specified burn intervals. The burn intervals correlate to specific dates when core inventory was altered. Fuel element material specifications for the burn interval (corresponding to the date of the validation data in Table 5.2) were used with the Neutronics Report MCNP model to develop peaking factors for the IFEs. The peaking factors and power levels from reactor operating records were used to calculate IFE power levels for TRACE calculations. The temperatures corresponding to

¹⁴ Neutronics Report

¹⁵ Derived from Neutronics Report, Figure 7, Current Core Power-Per-Element (in kW) Distribution at 1.1 MW

the location of the thermocouples in the IFEs were compared to operating data (Table 5.2). Comparison of the calculated and observed data indicates TRACE can predict steady-state behavior with reasonable accuracy (within $\pm 7.8\%$ of measured temperature values).

Table 5.2, TRACE CALCULATED AND IFE MEASURED FUEL TEMPERATURE COMPARISON

POSITION	FUEL ELEMENT	ELEMENT POWER (kW)	IFE INDICATED FUEL TEMP (°C)	TRACE CALCULATED FUEL TEMP (°C)	% DIFFERENCE BETWEEN MEASURED AND CALCULATED
INITIAL CONFIGURATION (12/18/2015)					
B03	10878	13.24	325	345	-5.80%
B06	10708	13.61	364	354	2.82%
IFE 10708 REPLACED WITH IFE 10809 (02/01/2016)					
B03	10878	13.30	319	346	-7.80%
B06	10809	15.30	420	394	6.60%

5.4 Pulsing Validation

There were over 300 pulses conducted at the UT TRIGA between initial criticality and 2016. Records of pulse data includes operator-calculated reactivity addition, control rod positions, core configuration (i.e., indicating the number of fuel elements in the core), peak power, total pulse energy, and peak temperature from the fuel temperature measuring channel. Pulses with reactivity values approaching \$1.00 have very large pulse widths, and assumption of adiabatic pulsing and a transient much smaller than some of the delayed neutron precursors decay constants may be affected by heat transfer.

The TRACE calculations were compared to historical data to validate the accuracy of the method used. Historical pulse data (reactivity addition, peak pulse power, and maximum temperature from the fuel temperature measuring channels) was compiled, with incomplete data purged. Figures 5.1 and 5.2 show the TRACE calculated power level and temperature compared to the historical data. While there is significant scatter in power level and temperature data with some outliers, the results overall show excellent agreement and provide a basis for validation.

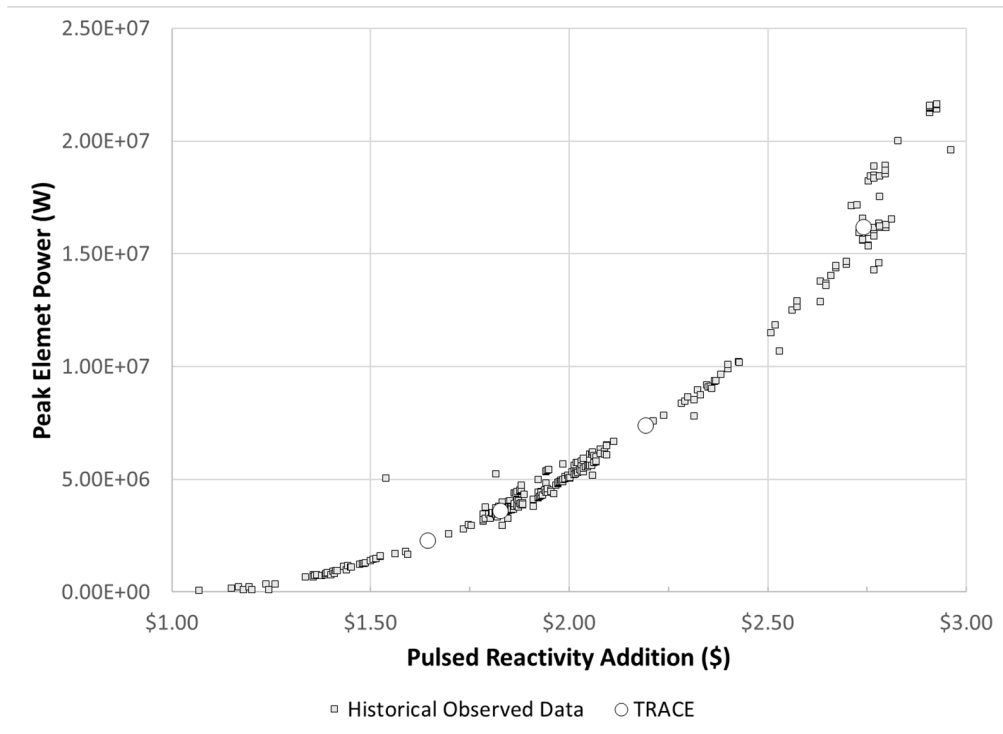


Figure 5.1: Peak Element Power Level Versus Pulse Reactivity Addition from UT TRACE Calculation Compared to Observed Historical Data

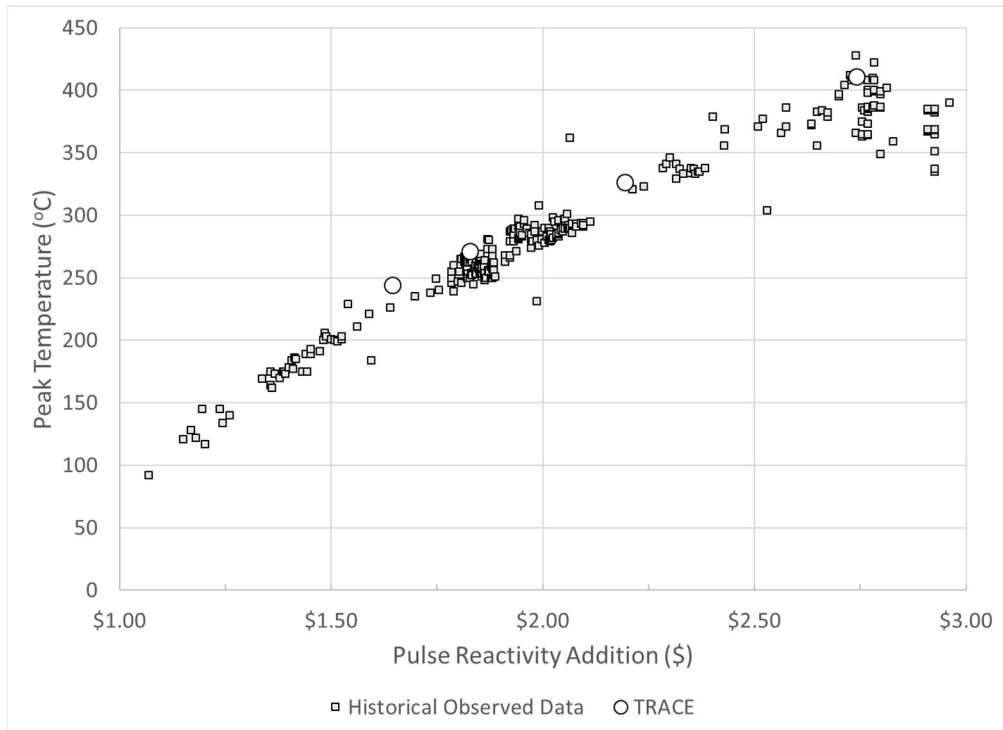


Figure 5.2: Peak Fuel Temperature Versus Pulse Reactivity Addition from UT TRACE Calculation Compared to Historical Data

Pulse records do not include factors that affect pulse characteristics such as initial fuel temperature, pool temperature, or recent operating history which might explain some of the scatter in the data. Although there is significant scatter and outliers in historical pulse power level data, it is clear that qualitatively the TRACE data agrees well with historical data. This indicates that TRACE can predict transient behavior with reasonable accuracy.

Average fuel element power and peak fuel temperature indicated from the IFE thermocouple location were compared to TRACE simulated values for pulses from \$1.25 to \$3.00 in \$0.25 increments. The results are shown in Table 5.3. As noted, the results show good agreement especially for pulses above \$2.00 in reactivity addition.

Table 5.3: Comparison of Observed Pulse Data with TRACE Simulation

Pulsed Reactivity $\delta k(\$)$	114 Element Core			TRACE Simulation		Deviation in Temperature (°K)	Deviation in Power (%)
	FT(°C)	FT(°K)	POWER (W)	TC (°K)	POWER (W)		
\$1.25	158	431.32	4.40E+05	410.58	3.49E+05	20.75	-26.04%
\$1.50	200	472.79	1.39E+06	460.50	1.23E+06	12.30	-12.73%
\$2.00	283	555.73	5.17E+06	547.79	4.76E+06	7.94	-8.50%
\$2.50	366	638.66	1.15E+07	627.83	1.08E+07	10.83	-6.12%
\$2.75	407	680.13	1.56E+07	668.99	1.49E+07	11.14	-4.77%
\$3.00	448	721.60	2.03E+07	716.87	1.95E+07	4.73	-4.18%

5.5 Conclusion on Model Validation

Fuel temperatures indicated by the fuel temperature measuring channels, and power and temperature from historical records of pulsing, were compared to data generated with TRACE calculations. The comparison demonstrates that the TRACE model predicts thermal hydraulic performance of the UT TRIGA reactor with reasonable accuracy.

6.0 Results

A limiting case and a nominal case were defined for analysis of the fuel element producing the maximum power in the core, based on Technical Specifications and parameters as identified in Table 4.2. The maximum peaking factor for the minimum number of fuel elements in the core was calculated in the Neutronics Report and used to identify and characterize the fuel element that produces the maximum power (and therefore the maximum power density). Table 5.1 values are used in LCC calculations except for the LCC Specific Values identified in Table 6.1

The maximum peaking factor for the LCC hot channel, i.e., channel producing the most power, is calculated as the ratio of the hot channel power to the average of the power of all elements based on the Neutronics Report (Figure 12 – Limiting Core Configuration Power-Per-Element Distribution at 1.1 MW). Reactor power is assumed to be 1.21 MW, the maximum licensed power with maximum instrument error identified in the 1992 Technical Specifications of 10%. The hot channel power is calculated using the peaking factor applied to the core power distributed over the number of fuel elements.

Table 6.1, LCC Specific Values

Physics Factors	Value
Prompt Neutron Generation Time	44 μ s
Core Radial Peaking Factor	1.68
Number of Fuel Elements ¹⁶	84
Maximum Hot Channel Power	24.34 kW
Pool Water Conditions	Value
Temperature	120.2 °C
Pressure	23.1 psia

Calculations of temperature across the fuel element were performed by TRACE in hot channel analyses. The results of temperature calculations are used to demonstrate that the maximum hot channel fuel temperature in limiting core conditions will remain less than 830°C for pulsing operations, 950°C if cladding is greater than or equal to 500°C, and 1150°C if cladding temperature is less than 500°C. The results of thermodynamic analysis for the hot channel were used in the Bernath correlation to demonstrate that the heat flux for the limiting and nominal cases will not result in departure from nucleate boiling for the hot channel.

6.1 Critical Heat Flux

TRACE was used to calculate heat transfer, water temperature, water density, pressure, and mass flow rate at 15 elevations in the heated length of the flow channel across a range of fuel element power levels (Table 6.2). These values were used to calculate the critical heat flux using the Bernath correlation (Eq. 4.27) with results illustrated in Fig. 6.1. The coolant mass flow rate is shown in Fig. 6.2. The radial and axial maximum fuel temperatures for the fuel element operating at the maximum power level are shown in Figs. 6.3 and 6.4, respectively.

Table 6.2, Steady State Calculations

Power kW	CHFR _{min}	Max Fuel Temp °C
11	5.82	367
14	4.45	414
17	3.56	459
20	2.94	502
23	2.48	559
24	2.39	559
24.34	2.37	564
27	2.43	599
30	2.26	639

¹⁶ Includes standard fuel elements, FFCRs and IFEs.

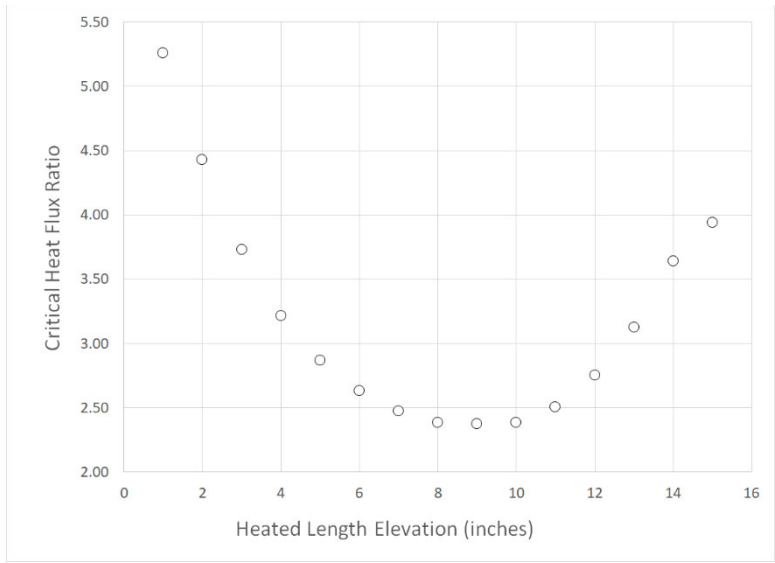


Figure 6.1: Critical Heat Flux, Bernath Correlation

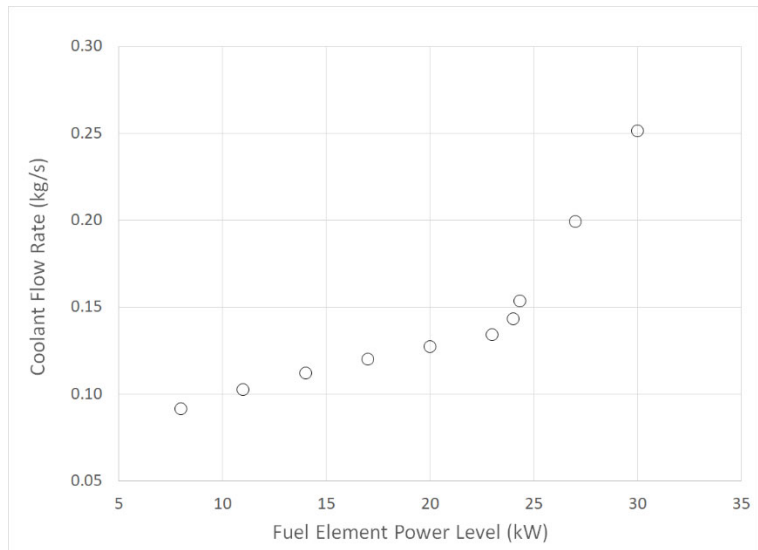


Figure 6.2: Coolant Flow Rate at Element Power

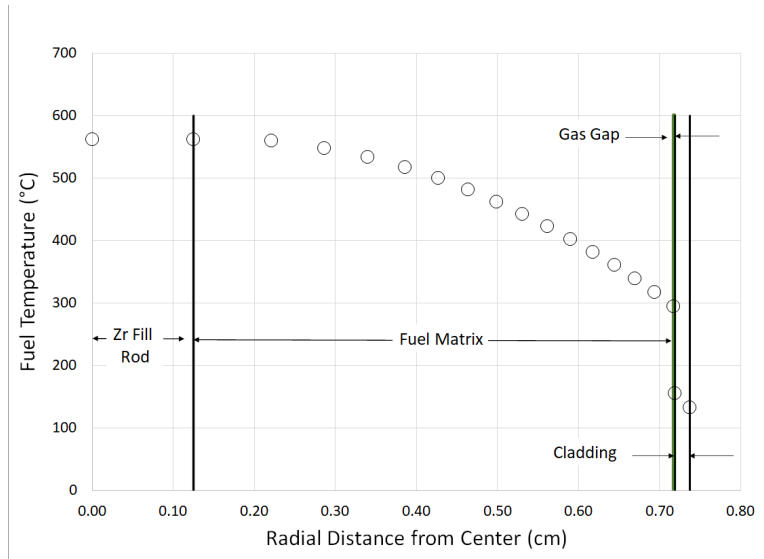


Figure 6.3, Hot Channel Radial Temperature Distribution

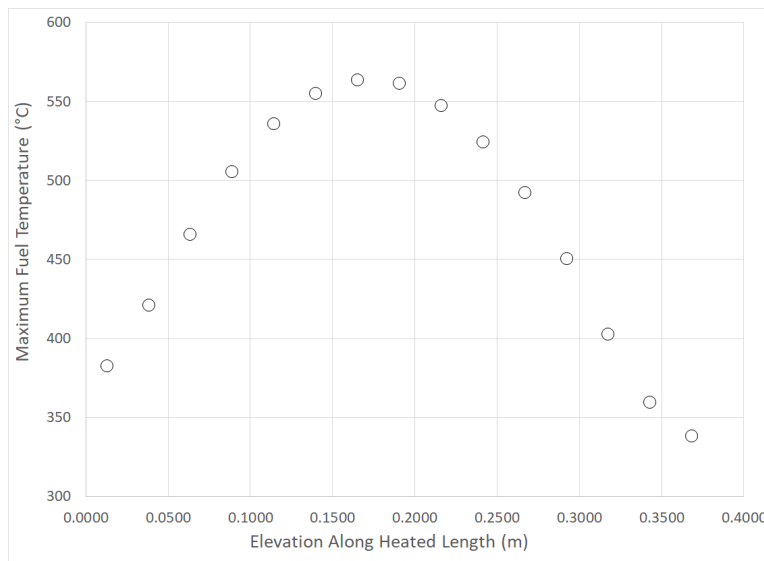


Figure 6.4: Hot Channel Axial Temperature Distribution

Limiting the critical heat flux ratio (CHFR) in the hot channel assures that departure from nucleate boiling will not occur. Therefore, CHFR minimum of 2.0 is not achieved at element power levels less than 30 kW, and operation at a maximum element power level of 24.34 kW has a sufficient margin to the 2.0 limit.

6.2 Pulsing from Low Power

Simulation of pulsing from shutdown power levels was performed. On initiation of a pulse, the ICS shifts instrumentation to a pulse monitoring mode for about 15 seconds. Pulsing reactivity calculations were performed in TRACE for the LCC hot channel using \$1, \$2, \$3, and \$4 insertions with initial conditions approximating shutdown power levels. The peak power as a function of pulsed reactivity is shown in Fig. 6.5 and the maximum fuel temperature is shown in Fig. 6.6.

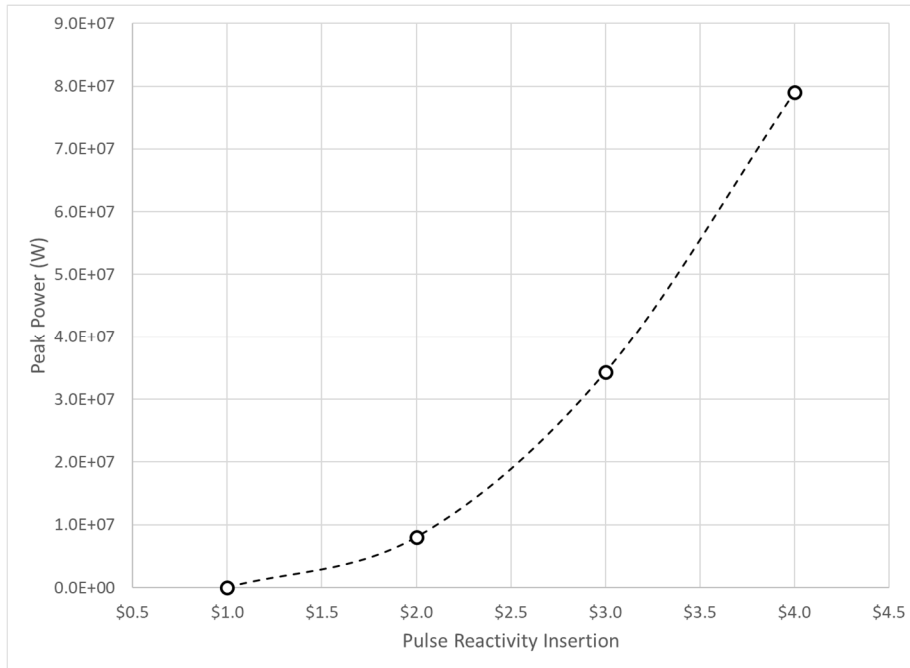


Figure 6.5: Hot Channel LCC Peak Power Level Versus Pulsed Reactivity Insertion of \$1, \$2, \$3 and \$4

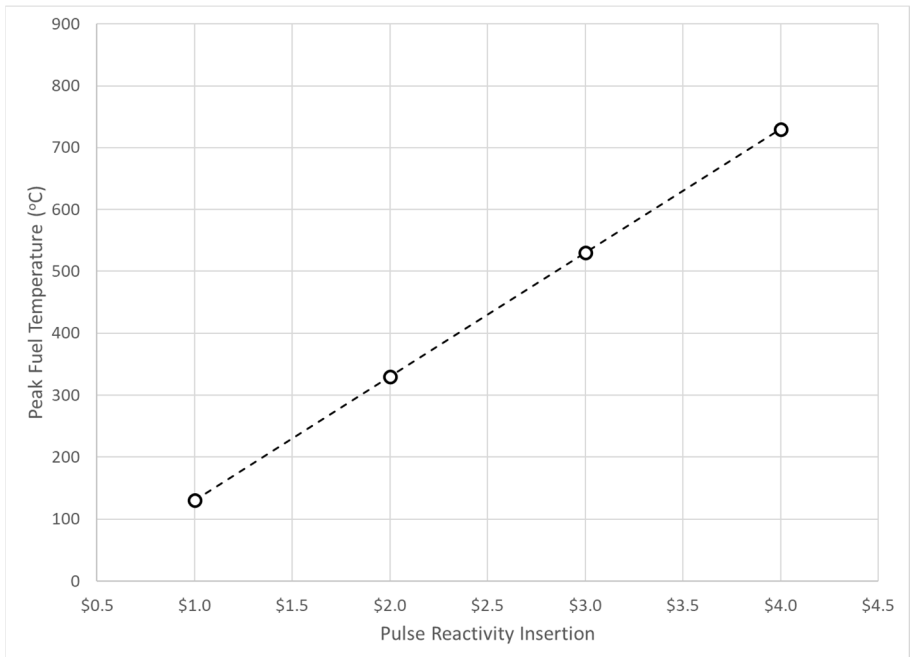


Figure 6.6: LCC Peak Fuel Temperature for Varying Reactivity Insertions

A \$3 insertion from low power levels (i.e., that do not generate sensible heat) resulted in a peak temperature of 530°C, with significant margin below the pulsing temperature limit. As shown in Fig. 6.6, the temperature limit was not exceeded for any reactivity insertions below \$4.

To study the pulsing limits in more detail, pulses from \$3 to \$4.40 were simulated in TRACE with the results given in Table 6.3. The pulse power, maximum fuel temperature, and fuel temperature at 3 locations in the fuel versus time following the pulse is shown in Fig. 6.7, 6.8, and 6.9, respectively.

Pulsed δk	Peak Power	Peak Temp.
\$	W	$^{\circ}\text{C}$
\$3.00	3.43E+07	530
\$3.50	5.51E+07	610
\$4.20	9.43E+07	778
\$4.30	1.01E+08	795
\$4.40	1.08E+08	824

For a maximum pulse of \$3.00, the peak maximum fuel temperature is 530 $^{\circ}\text{C}$ occurring near the thermocouple position about 13 seconds after the pulse. Temperature decreases after the peak.

Evolution of temperature is shown at the position adjacent to a thermocouple (position 4), an intermediate position (position 13) and position near the fuel outer surface (position 16) in Fig. 6.7. A pulse of \$4.40 reaches 824 $^{\circ}\text{C}$ in 15 seconds (Table 6.3) and is on an increasing trend.

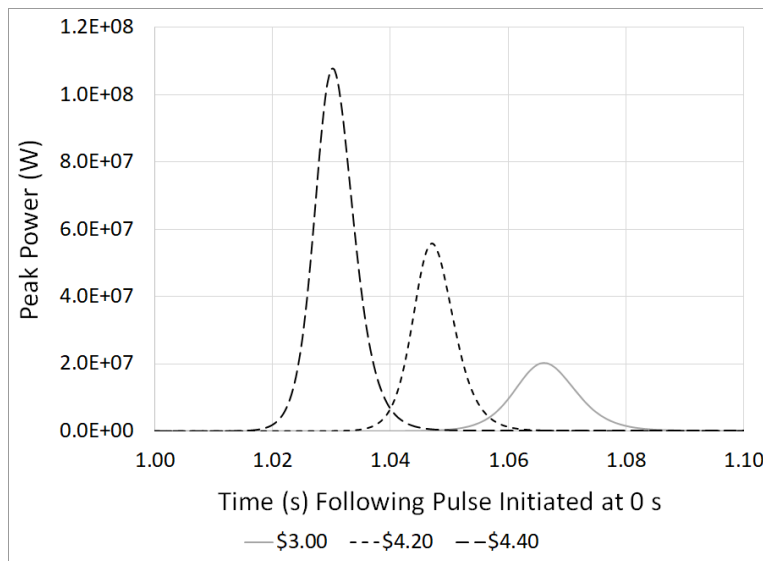


Figure 6.7: Peak Hot Channel Power Performance in Pulsing

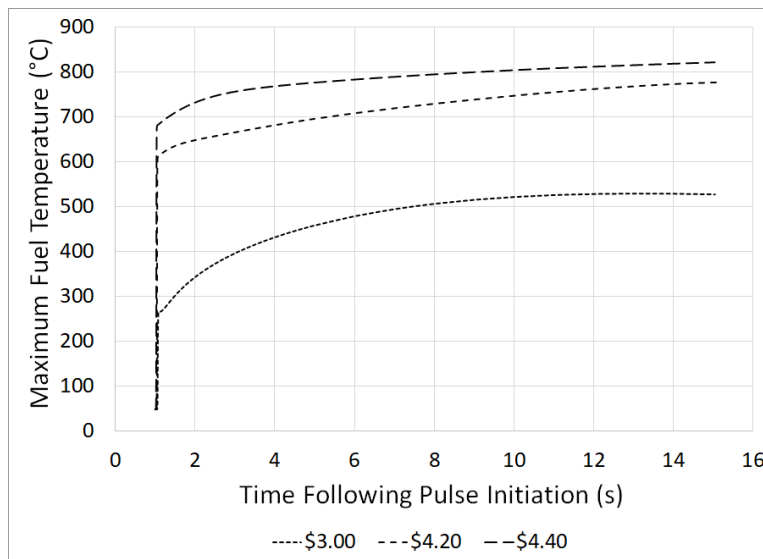


Figure 6.8: Maximum Hot Channel Temperature Performance in Pulsing

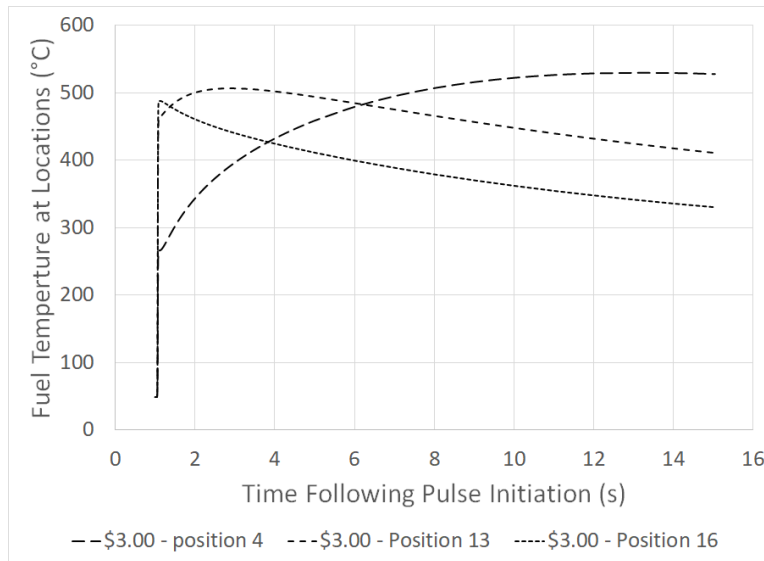


Figure 6.9: Evolution of Temperature for a \$3.00 Pulse, 3 Locations

Since pulsing to \$4.40 does not result in exceeding the temperature limit for pulsing, pulsing to \$3.00 will assure the fuel temperature remains below the 830°C limit by a large margin.

6.3 Pulsing from Power

Pulsing from power was simulated by a transient reactivity, with the reactivity applied to establish initial conditions for 200 seconds followed by the addition of \$3.00 of additional reactivity at 200 seconds. With initial element power level of 1.33 kW (corresponding to core power of 111 kW as indicated in Table 6.4, \$0.55 above the cold clean critical position), a \$3.00 pulse results in:

- maximum hot channel fuel temperature of 724 °C and
- final steady state power level of 24.02 kW.

Pulsing from an initial element power level of 2.08 kW (corresponding to core power of 174 kW, \$0.80 above the cold clean critical position), a \$3.00 pulse approaches the temperature limit, resulting in:

- maximum hot channel temperature of 826 °C and
- final steady state power level of 28.8 kW.

Table 6.4, Pulsing from Power Summary

Init Core Power (kW)	111 kW	124 kW	174 kW
Initial Ave. Element Power (kW)	1.33 kW	1.47 kW	2.08 kW
Final Element Power (kW)	24.02 kW	26.92 kW	28.80 kW
Final Core Power (kW)	1193 kW	1216 kW	1337 kW
Max Hot Channel Temperature (°C)	724 °C	747 °C	826 °C

Results for two cases approaching limits are shown in Fig. 6.10. Figure 6.10 shows the response for the average

fuel element (the bases for establishing core power level) and the hot channel peak temperature for the immediate response through the peak temperatures for initial core power levels of 111 kW and 174 kW. Figure 6.11 shows the long-term temperature response for initial core power of 111 kW, 124 kW (where the final steady-state power level will be 0.5% higher than the licensed power limit for steady state power operation), and 174 kW. In all cases, the peak temperatures occur 30-35 seconds following the pulse.

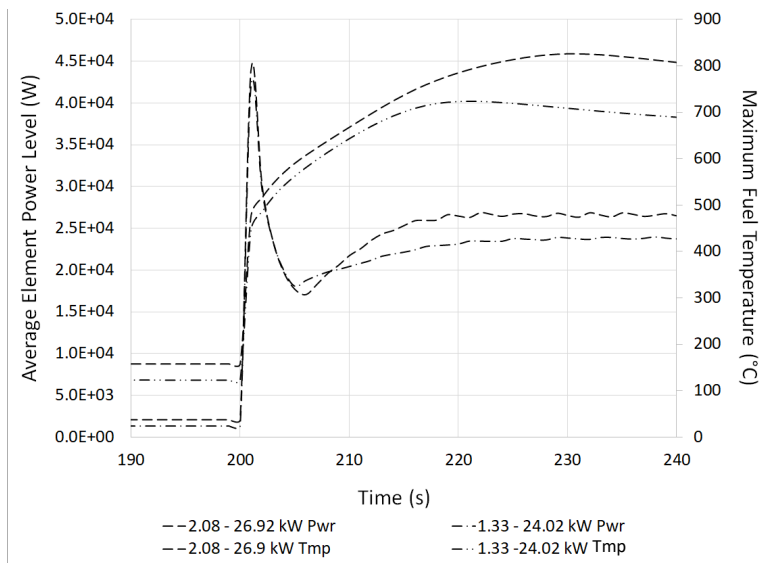


Figure 6.10, Responses to \$3.00 Pulse from Power within Maximum Pulse Temperature Limit (Transient) and Licensed Power Level (Steady State)

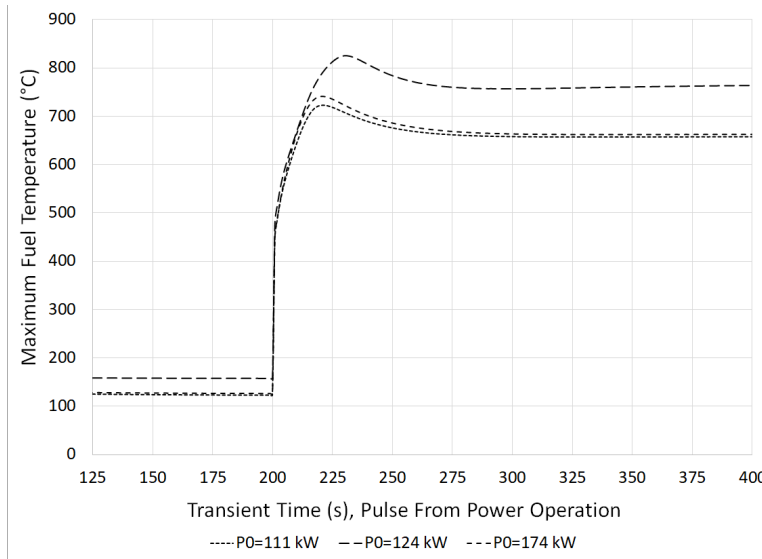


Figure 6.11, Temperatures Following Pulses from Power

If a pulse is initiated at 111 kW and allowed to come to equilibrium, the maximum hot channel power level is slightly less than the power for operation at the licensed power limit for steady-state power operation. If a pulse is initiated at 174 kW core power and allowed to come to equilibrium, although the pulsing temperature limit is met, the power level will be greater than the power for operation at the licensed power limit for steady-state power operation. At 30.0 kW, CHF_R has been shown to be greater than 2.0. However, a control rod interlock prevents pulsing if power level is greater than 1 kW. A TRACE calculation was performed with pulsing to 3.00 initiated from operations with core power at 1.021 kW ($3.95 \times 10^{-4} \Delta k/k$ compensating for temperature at power). The maximum hot channel fuel temperature for this transient is 522°C. A control rod inhibit interlock that prevents pulsing at greater than 1 kW is adequate by a large margin to ensure pulsing from power does not exceed the pulsing safety limit.

6.4 Analysis of Continuous Reactivity Addition from Full Power

An analysis of reactivity insertion at power was accomplished in three steps: (1) identification of the reactivity required to support full power operation at steady-state conditions (i.e., average fuel element power multiplied by 84 elements), (2) identify the time that the average fuel element operating at the reactivity in item 1 followed by a continuous reactivity addition reaches the scram setpoint, and (3) hot channel temperature response to a scram at varying continuous reactivity insertion rates, varying delays for scram initiation after reaching the LSSS, and one-second from initiation of scram to full insertion.

Reactivity insertions were varied to establish initial conditions of average element power corresponding to maximum licensed core power at the maximum error assumed in the 1992 Safety Analysis Report. A reactivity of 3.72 (0.0260 $\Delta k/k$) resulted in a steady-state core power of 1.258 MW, slightly higher than the nominal value, at 585 seconds of operation.

Calculations were performed for reactivity additions from the operating condition at various rates with varying scram-time delays (before the scram occurs after power reaches the scram setpoint). The minimum value for the reactivity addition rate is based on the 1992 Technical Specification for maximum control rod reactivity insertion rate (0.2% $\Delta k/k$ per second) up to 0.7% $\Delta k/k$ per second. The minimum value for scram response times is based on the 1992 Technical Specification value for full insertion no more than 1 second after initiation of the scram up to a maximum of 5 seconds. The shutdown reactivity values (-8.04, -

0.05628 $\Delta k/k$) were based on Neutronics Report values for the worth of all control rods (\$14.97) and the core excess reactivity (\$6.93). The 5 second delay at reactivity addition rates of 0.6% and 0.7% $\Delta k/k$ per second resulted in fatal run time errors.

Table 6.5, PEAK TEMPERATURE FOLLOWING CONTROL ROD FULL-INSERT DELAY

Reactivity addition rate	0.2%/s	0.4%/s	0.5%/s	0.6%/s	0.7%/s
Delay (seconds)	T_{max} ($^{\circ}C$)				
1	573	589	608	627	651
2	585	639	679	726	778
3	609	709	773	863	993
4	630	772	878	1050	1448
5	634	800	992	N/A	N/A

The maximum hot channel temperature during the transient was 573 $^{\circ}C$ for limiting conditions of the 1992 Technical Specifications. This is a conservative calculation, using an initial power level marginally higher than the maximum license power level with the maximum instrument error and a reactivity addition rate at the 1992 license limiting reactivity addition rate for control rods. A 4-second delay in scram initiation after power reaches 1.1 MW and does not exceed the safety limit. Therefore, a maximum scram setpoint of 1.1 MW is adequate to prevent exceeding the safety limit for an event where a continuous reactivity addition occurs while operating at full power with the maximum power level instrument error and a maximum reactivity rate of 0.2% $\Delta k/k \cdot s^{-1}$ with a maximum of 1 second for full insertion of control rods.

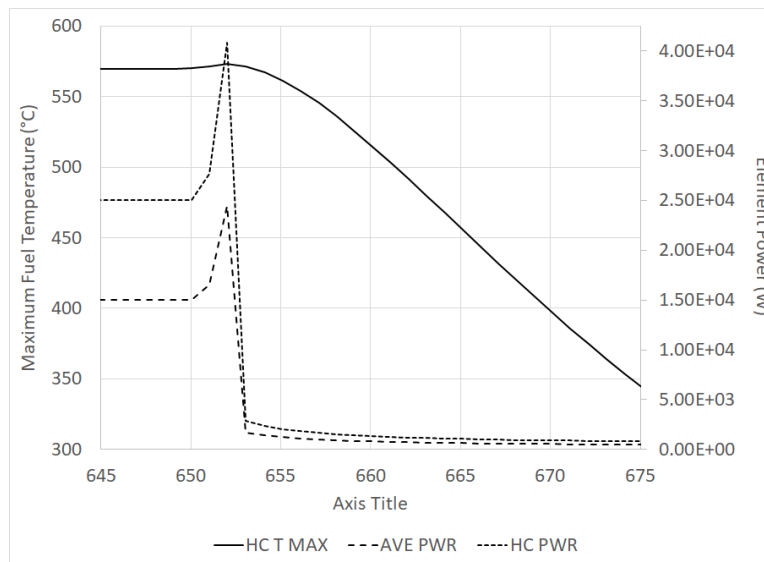


Figure 6.12, Response to 0.2% $\Delta k/k$ per Second Reactivity Addition at Full Power, Full Control Rod Insertion 1 Second after 1.1 MW

6.5 Loss of Coolant Event (LOCA)

The LOCA analysis was a 2-step process with first a TRACE calculation to establish initial conditions at 25 kW per element with a series of shutdown and decay intervals with water cooling. This was followed by a TRACE restart case initiated as a transient calculation with air cooling. Air temperature was assumed to be 77°F. The method of ANSI/ANS-5.1-2014, Decay Heat Power in Light Water Reactors was used to evaluate fission and fission product power decay in time. Four cases were calculated (Table 6.6) using four intervals between shutdown and instantaneous replacement of water cooling with air cooling. The time-dependent behavior is shown in Fig. 6.15 over four hours following shutdown. The maximum cladding temperature occurred with 1 s delay before air cooling, and was 784°C. Therefore, on a loss of cooling event following steady-state operation at 25 kW per element, the maximum fuel temperature remains at acceptable levels.

Table 6.6, LOSS OF WATER-COOLING ANALYSIS

DELAY FOR AIR COOLING (s)	MAXIMUM TEMPERATURE (°C)
1	787
60	780
600	753
1200	733

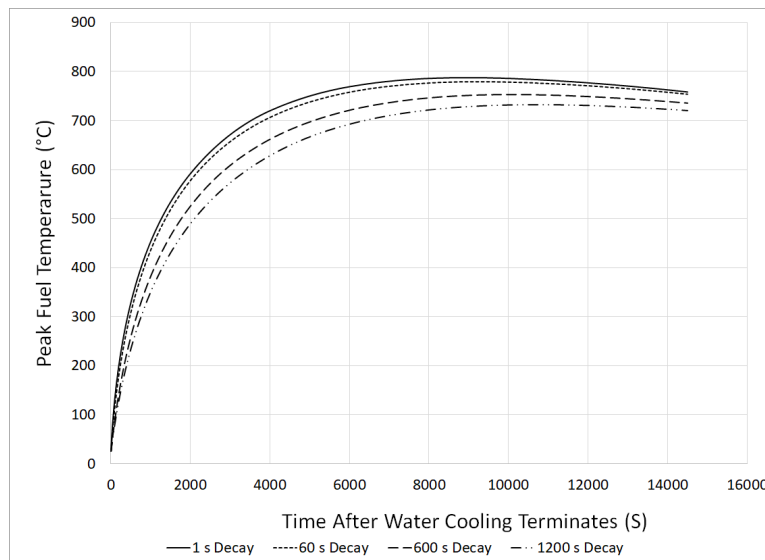


Figure 6.13, Maximum Fuel Temperature with Loss of Cooling Following Steady-State Operation at 25 kW Per Element

7.0 Summary

The minimum LCC is 84 elements for steady-state operations at 1210 kW (the licensed limit with maximum measuring channel error). A summary of the results from the thermal-hydraulics analysis for the LCC is given in Table 7.1. The following conclusions are made:

1. Power levels up to 1210 kW demonstrate that a minimum CHF of 2.0 is assured in the limiting core configuration (minimum pool water level, maximum pool temperature).
2. Pulsing from shutdown to 3.00 will remain within the pulse temperature limit. Pulsing to 3.00 from operation at power levels up to 174 kW will result in maximum fuel temperatures that remain within

- the pulse temperature limit.
3. Fuel temperature during continuous reactivity addition from full power operations for delays in control rod insertion up to 3 seconds at reactivity addition rates up to 0.7% $\Delta k/k$ per second will remain within the steady-state temperature limit.
 4. Fuel temperatures following a loss of coolant after steady-state operation will remain within limits.

Table 7.1: Final Summary

Analysis	Value	Max/Min	Limit
Steady State Power Level	24.34 kW per element	564 °C 2.37 (CHFR)	950°C /1150°C 2.0 (CHFR)
Reactivity Transients			
Pulse from Shutdown	\$3.00	530°C	830°C
Pulse from Operation	\$3.00 1.02kW	522°C	830°C
Continuous Reactivity Addition from Full Power	0.2% $\Delta k/k/s$ 1 s scram	573°C	1150°C
Loss of Coolant Event	25.00 kW per element ¹⁷	787°C	950°C

¹⁷ Initial Steady State Condition